

Reviewed Preprint

v1 • March 25, 2026

Not revised

Reviewed Preprint

v2 • April 22, 2026

Revised by authors

✉ For correspondence:

jjex@umich.eduxiaoqiah@umich.edu

Competing interests: No

competing interests declared

Funding: See [page 33](#)Reviewing editor: Martin Graña,
Institut Pasteur de Montevideo,
Uruguay

© 2026, Xiong et al. This article is distributed under the terms of the [Creative Commons Attribution License](#), which permits unrestricted use and redistribution provided that the original author and source are credited.

Fully computational design of PAM-relaxed *Staphylococcus aureus* Cas9 with expanded targeting capability using UniDesign

Youcai Xiong¹, Li-Kuang Tsai¹, Jun Zhou¹, Shuang Chen¹, Xiaofeng Xia², Jifeng Zhang¹, Y Eugene Chen¹, Jie Xu¹ ✉, Xiaoqiang Huang¹ ✉¹Center for Advanced Models for Translational Sciences and Therapeutics, Department of Internal Medicine, University of Michigan Medical School, Ann Arbor, United States • ²Research & Development, ATGC Inc., King of Prussia, United States

eLife Assessment

This **important** study demonstrates the power of the UniDesign computational framework in prospectively engineering a PAM-relaxed *Staphylococcus aureus* Cas9 variant with editing performance comparable to evolution-derived counterparts. The authors responded promptly and thoroughly to reviewer concerns and strengthened the manuscript with additional experimental validation, providing **compelling** evidence through expanded biochemical characterization across multiple human cell types, comprehensive deep-sequencing analyses, and direct comparisons with established variants that illuminate the mechanistic basis of PAM specificity remodeling and Cas9 optimization. By establishing computational design as a rigorous and viable alternative to directed evolution for CRISPR systems, this work will be of broad interest to the protein engineering, genome engineering, synthetic biology, and computational protein design communities.

<https://doi.org/10.7554/eLife.110906.2.sa4>

Abstract

CRISPR–Cas9 nucleases have transformed genome engineering, yet their application is often constrained by protospacer-adjacent motif (PAM) requirements. *Staphylococcus aureus* Cas9 (SaCas9) is particularly attractive for in vivo applications due to its compact size; however, its NNGRRT PAM limits targetable genomic sites. Here, we report KRH, a SaCas9 variant designed entirely from the wild-type enzyme through a fully computational point-mutation design workflow, UniDesign, without additional experimental optimization. As expected, KRH efficiently recognizes an expanded NNNRRT PAM and exhibits substantially enhanced editing efficiency at non-canonical PAM sites, with improvements of up to 116-fold over the wild type. KRH achieves genome- and base-editing efficiencies comparable to, or exceeding, those of the well-known evolution-derived KKH variant. Computational modeling by UniDesign provides a mechanistic explanation for the PAM relaxation observed in both KRH and KKH, with structural and energetic analyses revealing that KRH relaxes PAM specificity by fine-tuning the balance between sequence-specific interactions with PAM bases and nonspecific contacts with the DNA backbone. Beyond its practical utility, KRH demonstrates that computational design can identify a minimal set of mutations sufficient to remodel the PAM interface while preserving high nuclease activity. This approach recapitulates—and in some cases surpasses—the performance of evolution-derived

variants, offering a scalable strategy for high-throughput Cas9 engineering. Overall, these results establish KRH as a blueprint for rationally engineered, PAM-relaxed nucleases and underscores the power of computational design to accelerate next-generation genome editing.

Introduction

Clustered regularly interspaced short palindromic repeats (CRISPR) and their associated nucleases have revolutionized biological research and therapeutic genome engineering (Doudna and Charpentier, 2014 [↗](#); Hsu et al., 2014 [↗](#); Komor et al., 2017 [↗](#); Huang et al., 2022 [↗](#)). Among these systems, *Staphylococcus aureus* Cas9 (SaCas9) is particularly attractive due to its compact size, which facilitates efficient packaging into adeno-associated virus (AAV) vectors for in vivo delivery (Ran et al., 2015 [↗](#)). However, the utility of SaCas9 is constrained by its relatively restrictive protospacer-adjacent motif (PAM) requirement, NNGRRT, which limits the number of targetable genomic loci (Nishimasu et al., 2015 [↗](#)). Expanding SaCas9 PAM compatibility while retaining high editing efficiency remains a key challenge for both therapeutic and biotechnological applications.

Previous efforts to relax SaCas9 PAM specificity have relied on molecular evolution, evolution-based chimera engineering, or combined computational–experimental strategies (Kleinstiver et al., 2015 [↗](#); Luan et al., 2019 [↗](#); Ma et al., 2019 [↗](#)). The well-known E782K/N968K/R1015H (KKH) variant, generated through iterative mutagenesis and selection, broadens PAM recognition to NNNRRT (Kleinstiver et al., 2015 [↗](#)). Despite its effectiveness, this approach does not leverage structural information and therefore provides limited mechanistic insight into PAM relaxation. Similarly, chimera engineering method successfully produced chimeric SaCas9 (cCas9) variants with altered recognition of noncanonical PAM sequences such as NNVRN and NNVACT (Ma et al., 2019 [↗](#)), but offered little understanding of the underlying molecular determinants. A combined computational–experimental approach (COMET) explained the activity of KKH and proposed new variants targeting NNGRRN (Luan et al., 2019 [↗](#)); however, its reliance on intensive molecular dynamics simulations and free-energy perturbation calculations makes it computationally expensive and impractical for high-throughput variant screening.

In our previous work, we demonstrated that UniDesign, a general computational protein design framework, can efficiently and accurately model PAM recognition across diverse Cas9 and Cas12 enzymes (Huang et al., 2023b [↗](#)). When native PAM-interacting amino acids (PIAAs) were preserved, UniDesign recovered predicted natural PAMs; conversely, when natural PAMs were fixed, UniDesign redesigned PIAAs recapitulated native PIAA residues with 86% sequence similarity (Huang et al., 2023b [↗](#)). These results indicated that UniDesign can capture the intrinsic coupling between PAMs and their interacting residues, suggesting its potential for rationally engineering SaCas9 variants with expanded PAM compatibility.

Here, we report KRH (E782K/N968R/R1015H), a new SaCas9 variant designed entirely in silico using an improved UniDesign workflow for efficient point-mutation generation, without any additional wet-lab optimization. Genome editing and base editing experiments show that KRH robustly recognizes the expanded NNNRRT PAM, matching the relaxed specificity of KKH. Notably, KRH exhibits comparable or superior editing activity across multiple genomic contexts, underscoring its practical utility as a fully computationally designed alternative to evolution-derived variants.

Because KRH was generated exclusively through computational design, our approach also enables detailed interrogation of the structural and energetic mechanisms underlying PAM recognition. Modeling analyses reveal (1) how the KRH substitutions enhance PAM compatibility, (2) how both KRH and KKH achieve PAM relaxation through related yet distinct molecular interactions, and (3) a minimal set of mutations sufficient to remodel the PAM interface without substantially compromising nuclease function. These insights highlight the advantages of UniDesign for rationally CRISPR nuclease engineering.

Together, this work establishes KRH SaCas9 as a powerful, computationally designed nuclease with broadened PAM recognition and demonstrates how atomic-level modeling can both guide and mechanistically explain precise modifications to the PAM-interacting interface. Our results

underscore the growing potential of computational protein design approaches like UniDesign to complement traditional molecular evolution strategies for next-generation genome editor engineering.

Results

Improving UniDesign for computational point-mutation variant design

UniDesign is a general framework for computational protein design, and we have demonstrated its effectiveness across a wide range of design and modeling tasks (Huang et al., 2023a [↗](#); Huang et al., 2023b [↗](#)). In its standard workflow, UniDesign builds rotamers at selected design sites on the input protein scaffold, scores combinations of rotamers using the UniEF energy function (Huang et al., 2023a [↗](#); Huang et al., 2023b [↗](#)), and identifies low-energy sequences using simulated annealing Monte Carlo (SAMC) search (Huang et al., 2020 [↗](#)) (Figure 1A [↗](#), light blue). Low-energy sequences from independent trajectories are then collected for downstream analysis.

Although the standard pipeline works well for de novo sequence design and applications that do not restrict the number of mutations—for example, exploring entirely new amino-acid combinations across many positions—it is less suitable for designing variants with only a small, desired number of point mutations, which is often preferred for practical experimental reasons. As a result, in earlier work with UniDesign we had to manually adjust mutable sites one at a time to perform in silico site-directed saturation mutagenesis of CYP201A1 to identify stereoselective point mutations and then combined them (Huang et al., 2023a [↗](#); Sun et al., 2026 [↗](#)).

Another challenge is redundancy: identical low-energy designs frequently recur across independent SAMC trajectories, reducing design diversity. For example, a particularly favorable single mutant may be sampled repeatedly, sometimes dozens of times, crowding out other potentially informative variants and limiting exploration of the local sequence landscape.

To address these issues, we improve UniDesign's mutant-generation strategy by constraining the number of mutations allowed during SAMC simulations (Figure 1A [↗](#), dark blue). Designs with mutation counts outside the desired range receive a large penalty, biasing the search toward sequences with the specified number of mutations (see Methods). Although this ensures that designs have the intended mutation count, we found that UniDesign still often produced the same low-energy variants multiple times. To reduce this redundancy, we introduced an additional constraint that penalizes any design whose sequence is identical to one already reserved, ensuring that each low-energy design produced by a SAMC trajectory is unique (see Methods). With these two improvements, the enhanced UniDesign pipeline can reliably generate a variety of point-mutation variants (e.g., single, double, or triple mutants) in each run. Nevertheless, because SAMC remains stochastic, multiple runs are still required to obtain sufficient variants and assess design-space convergence.

Iterative computational design of SaCas9 variants to relax PAM requirements

In our previous work, we showed that UniDesign-derived binding energies correlate strongly with PAM–PIAA interactions: wild-type (WT) PIAAs preferentially recognize canonical PAMs, and native PAMs favor WT PIAAs (Huang et al., 2023b [↗](#)). Building on this rationale, we used the enhanced UniDesign pipeline to iteratively design SaCas9 variants with relaxed PAM specificity. WT SaCas9 recognizes the NNGRRT PAM; here, our objective was to expand this specificity to NNNRRT. Using the SaCas9–sgRNA–DNA complex structure (Protein Data Bank (PDB): 5AXW; PAM: TTGGGT) (Nishimasu et al., 2015 [↗](#)) as the design scaffold, we considered four representative PAMs for PAM-relaxation design: TTAGGT, TTCGGT, TTGGGT, and TTTGGT.

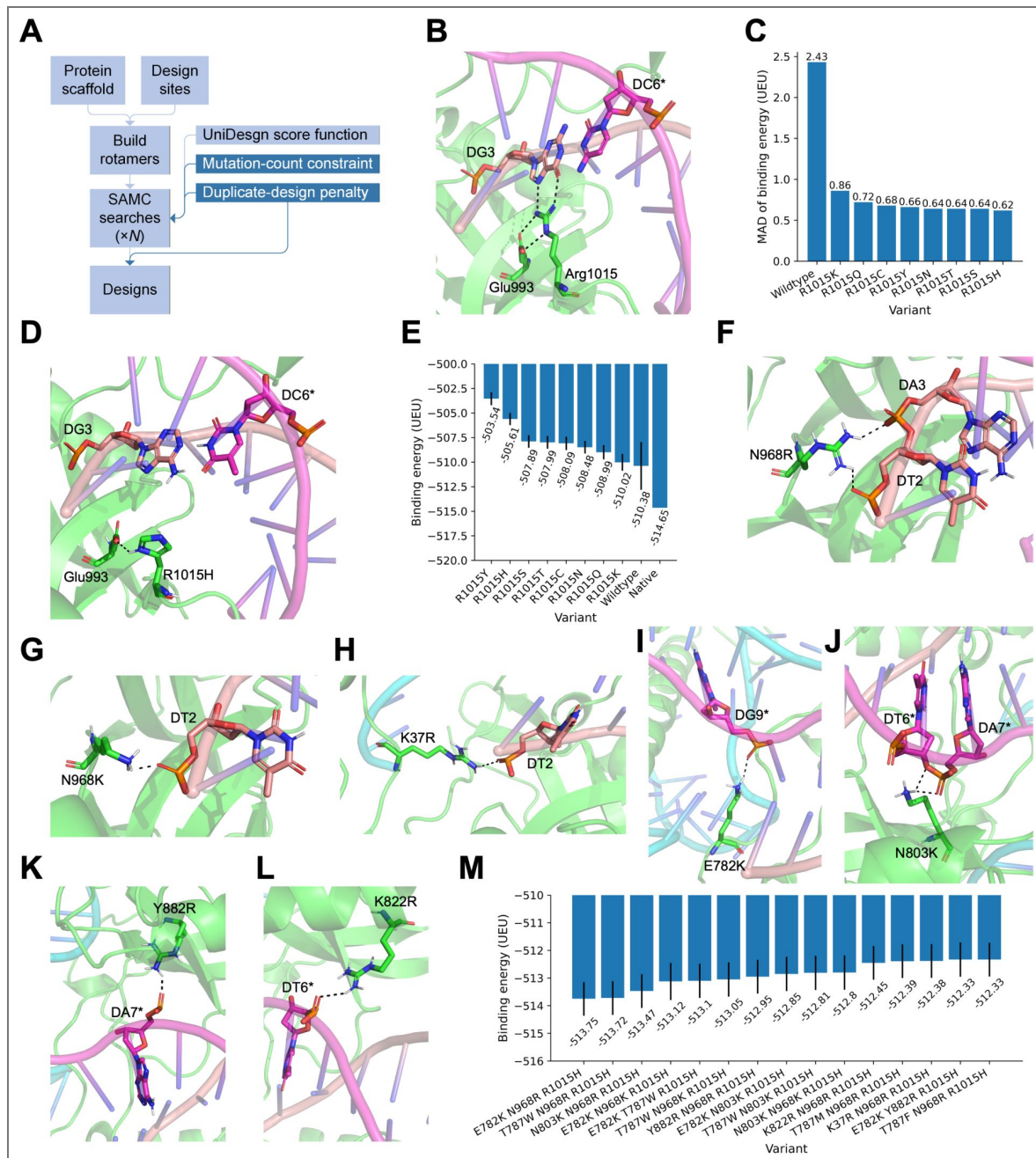


Figure 1. Computational design of PAM-relaxed *Staphylococcus aureus* Cas9 variants.

(A) Improved UniDesign workflow for point-mutation generation. (B) Specific recognition of the third guanine in the NNGRRT PAM by Arg1015, positioned through salt-bridge interaction with Glu993. Non-target strand (NTS) nucleotides are indicated by asterisks (as in subsequent panels). (C) Mean absolute deviation (MAD) of binding energies across four PAMs (TTAGGT, TTCGGT, TTGGGT, and TTTGGT) for substitutions of Arg1015 with polar or positively charged residues. (D) UniDesign model of the R1015H mutant, showing His1015 forming a hydrogen bond with Glu993. (E) Mean binding energy across the four PAMs for substitutions of Arg1015 with polar or positively charged residues; error bars represent MADs. (F–L) UniDesign models of mutations: N968R (F), N968K (G), K37R (H), E782K (I), N803K (J), Y882R (K), and K822R (L). (M) Mean binding energies of the top triple-mutant variants across the four PAMs; error bars represent MADs.

First design iteration: reducing positional bias at PAM position 3

We began by targeting Arg1015, which specifically recognizes the third guanine of NNGRRT (Nishimasu et al., 2015) via bidentate hydrogen-bonding interactions (Figure 1B). For the TTGGGT PAM, WT SaCas9 achieved a binding energy of -514.65 UniDesign energy units (UEU) for TTGGGT, markedly lower than for the other three PAMs (Data S1), confirming the central role of Arg1015 in this positional preference.

Because binding energy is a major determinant of PAM recognition (Huang et al., 2023b), we hypothesized that mutations producing similar binding energies across all four PAMs would promote relaxed PAM specificity. To quantify this similarity, we calculated the mean absolute deviation (MAD):

$$MAD = \frac{1}{n} \sum_{i=1}^n |e_{\text{bind}}^i - \mu|, \quad \mu = \frac{1}{n} \sum_{i=1}^n e_{\text{bind}}^i$$

where e_{bind}^i is the binding energy of a SaCas9 variant for the i -th PAM and μ is the mean binding energy for all n PAMs. A MAD of zero indicates identical binding energies.

WT SaCas9 had a high MAD of 2.43 UEU across the four PAMs (Figure 1C). To reduce this bias, we performed a single-mutant scan at position 1015, sampling polar and positively charged amino acids (Cys, His, Lys, Asn, Gln, Arg, Ser, Thr, and Tyr). All substitutions substantially reduced the MAD to 0.62–0.86 UEU (Figure 1C). Among these, R1015H emerged as a promising substitution because: (1) it achieved a low MAD of 0.62 UEU, indicating effective reduction of positional bias, and (2) histidine, like arginine, can carry a positive charge near physiological pH and can be stabilized by Glu993 via hydrogen-bonding interaction (Figure 1D), helping maintain a similar electrostatic environment to the WT. However, the mean binding energy of R1015H (-505.61 UEU) was approximately 9 UEU weaker than the WT for TTGGGT (-514.65 UEU) (Figure 1E), suggesting that R1015H alone may not provide sufficiently strong, generalizable DNA binding across TTGGGT PAMs.

Second design iteration: restoring binding via nonspecific interactions

To recover binding strength while avoiding sequence-dependent effects, we next introduced additional mutations aimed at enhancing nonspecific protein–DNA interactions. We generated double mutants consisting of R1015H plus one additional mutation at the remaining mutable sites. Across all four PAMs, UniDesign identified 487 double mutants with mean binding energies ranging from -509.77 to -485.86 UEU (Data S2). Of these, 37 variants showed both a mean binding energy < -507.61 UEU and a MAD < 0.82 UEU.

Structural analysis revealed that many low-energy designs (e.g., D786Q/M/I/L/V/N; S908R/K/M/I/W; N885F/Y/M/R; T1019L; E782R/T; N785L/K/R/M) primarily enhanced contacts with DNA or sgRNA bases rather than the DNA backbone. Likewise, the E993S/P/A/G/K/R variants relieved some steric clashes between His1015 and the thymine at the second PAM position by altering His1015 geometry, but simultaneously disrupted the favorable, preorganized His1015–Glu993 hydrogen bond (Figure 1D). These patterns indicated that such substitutions might not support generalizable PAM relaxation.

In contrast, another subset of double mutants formed favorable backbone-mediated, DNA sequence-nonspecific interactions. These included mutations such as N968R/K, E782K, T787W/F/M, N803K/W, Y882R, K37R, and K822R. These positively charged arginine or lysine residues were capable of forming salt bridges with DNA backbone phosphate groups (Figure 1F–L), while the bulky hydrophobic residues could form favorable packing interactions (Figure S1). These variants achieved binding energies between -507.76 UEU (N803W/R1015H) and -509.70 UEU (N968R/R1015H) (Data S2), although none matched the WT energy of -514.65 UEU for the native TTGGGT PAM.

Third design iteration: combining favorable substitutions

To further strengthen binding, we generated triple mutants by combining promising double-mutant substitutions. Across all four PAMs, UniDesign produced 50 triple mutants, all of which had lower mean binding energies than their corresponding double mutants, indicating largely additive

energetic contributions (Data S3). The top-performing designs combined E782K, N968R/K, T787W, N803K, or Y882R with R1015H. The best triple mutant, E782K/N968R/R1015H (denoted KRH), achieved a mean binding energy of -513.75 UEU and a MAD of 0.61 UEU, closely matching the WT energy for TTGGGT (-514.65 UEU) (Figure 1M [↗](#)). The previously reported KKH variant (E782K/N968K/R1015H) was also recapitulated and ranked fourth by mean binding energy (-513.12 UEU; MAD 0.67 UEU). Other top-ranked variants included T787W/N968R/R1015H, N803K/N968R/R1015H, and E782K/T787W/R1015H (Figure 1M [↗](#); Data S3).

Because the known KKH variant exhibits strong editing activity across NNGRRT PAMs (Kleinstiver et al., 2015 [↗](#))—and given the close structural and energetic similarity between KKH and our top-ranked KRH variant—we anticipated that KRH may display comparable or superior genome-editing performance. We therefore proceeded to experimental assessment without an additional design iteration.

KRH expands the targeting range of SaCas9 across diverse cell types

To systematically evaluate whether the computationally designed KRH variant can expand the PAM range from NNGRRT to NNNRRT, we compared the editing efficiencies of WT and KRH SaCas9 across multiple genomic targets with distinct PAM sequences.

In HEK293T cells, KRH showed markedly improved editing efficiency compared to the WT at non-canonical PAM sites (NNHRRT, H=A/C/T) (Figure 2A [↗](#)). The enhancement ranged from 1.4-fold to 116.3-fold. For example, at the *RUNX1* locus, editing efficiency increased from 0.47% with SaCas9 to 54.68% with KRH, a 116.3-fold improvement. Although efficiency at a classical NNGRRT PAM site (*VEGFA*) modestly decreased from 80.19% (WT) to 67.37% (KRH), overall activity remained high. These results indicate that KRH broadens the PAM compatibility of SaCas9 while maintaining strong activity at canonical PAMs.

To assess whether this PAM-relaxing effect is generalizable across cell types, we next compared KRH and WT SaCas9 in A549, HeLa, and U2OS cells using targets with various PAM sequences (Figure 2B–D [↗](#)). In all three cell types, KRH exhibited significantly higher editing efficiencies at non-classical PAM sites while maintaining comparable activity to WT at classical NNGRRT sites. Editing efficiencies varied among cell types, suggesting that SaCas9 activity is influenced by cellular context; nevertheless, KRH consistently outperformed WT at non-classical PAMs (Figure 2E [↗](#)). On average, KRH increased editing efficiency by 5.4-fold in HEK293T cells, 4.3-fold in A549 cells, 6.9-fold in HeLa cells, and 8.4-fold in U2OS cells.

We also compared the performance of KRH and WT SaCas9 across different PAM categories (Figure 2F [↗](#)). At NNARRT, NNCRRRT, and NNTRRT PAMs, KRH improved editing efficiency by an average of 3.3-fold, 10.9-fold, and 15.4-fold, respectively. At canonical NNGRRT PAMs, KRH generally retained activity comparable to WT SaCas9.

Taken together, these results demonstrate that the computationally designed KRH SaCas9 variant substantially broadens the PAM range of WT SaCas9 and enables efficient genome editing at sites with non-classical PAM sequences across multiple human cell types.

KRH SaCas9-based adenine base editor (ABE) broadens base-editing capabilities

Given that KRH expands the PAM compatibility of SaCas9, we next examined whether a base editor engineered from KRH could target a broader set of genomic regions. To this end, we constructed KRH-ABE by fusing the ABE8e (V106W) deaminase to the N-terminus of KRH nickase (D10A) (Richter et al., 2020 [↗](#)). For an appropriate comparison, we also generated a WT SaCas9 (D10A)-based ABE, termed WT-ABE. We then systematically compared the editing efficiencies of WT-ABE and KRH-ABE across four cell types (HEK293T, A549, HeLa, and U2OS) at genomic loci bearing diverse PAM sequences.

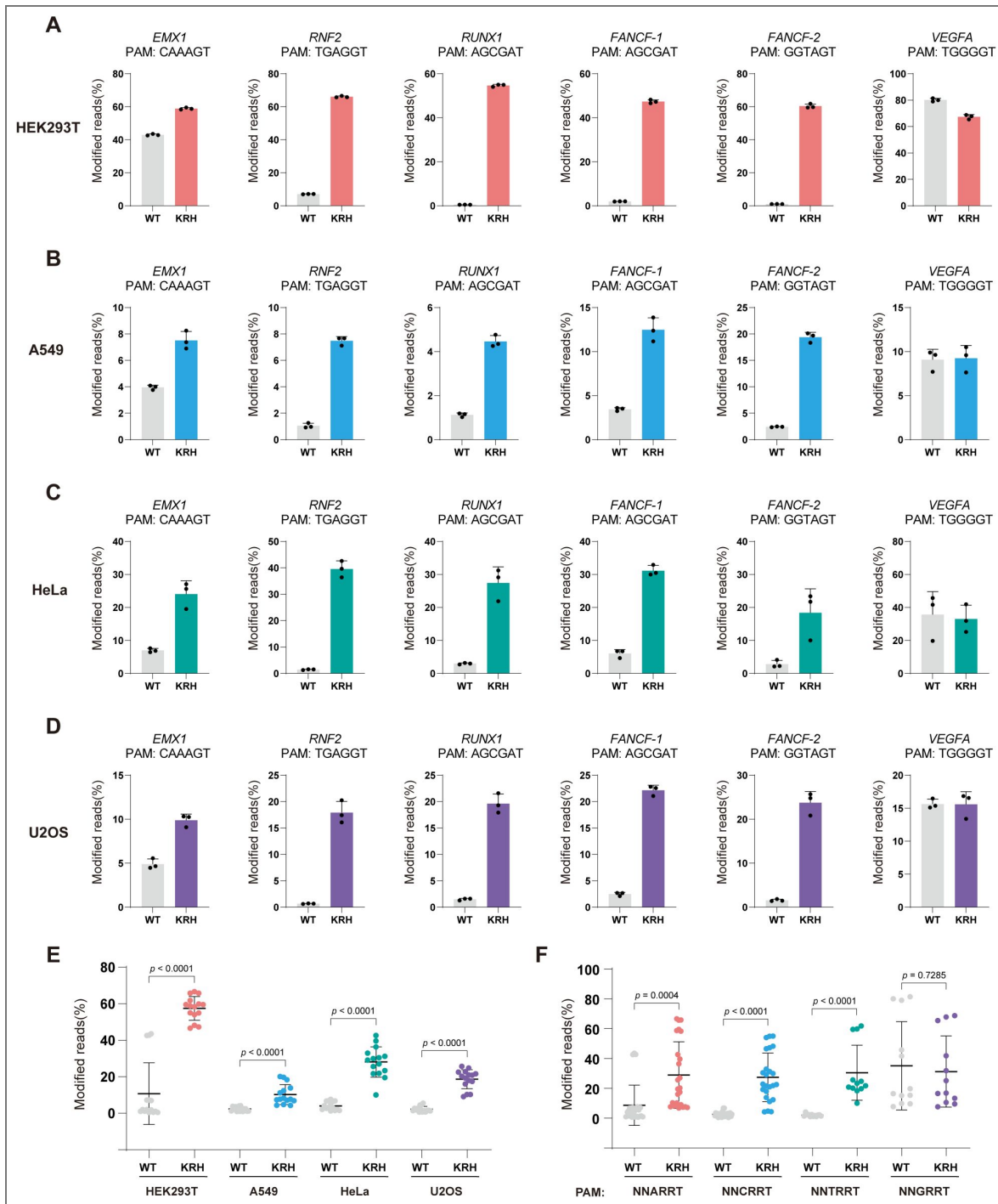


Figure 2. KRH expands the targeting range of SaCas9 across diverse cell types.

(A) Editing efficiencies of wild-type (WT) SaCas9 and the KRH variant at different PAM sites in HEK293T cells. Bars represent the mean of $n = 3$ independent biological replicates; error bars indicate s.d. (B) Editing efficiencies of WT SaCas9 and the KRH variant at different PAM sites in A549 cells. Bars represent the mean of $n = 3$ independent biological replicates; error bars indicate s.d. (C) Editing efficiencies of WT SaCas9 and the KRH variant at different PAM sites in HeLa cells. Bars represent the mean of $n = 3$ independent biological replicates; error bars indicate s.d. (D) Editing efficiencies of WT SaCas9 and the KRH variant at different PAM sites in U2OS cells. Bars represent the mean of $n = 3$ independent biological replicates; error bars indicate s.d. (E) Statistical comparison of editing efficiencies between WT SaCas9 and the KRH variant at non-canonical PAM sites across HEK293T, A549, HeLa, and U2OS cells. Data are shown as mean \pm s.d.; statistical significance was assessed using a two-tailed unpaired Student's t -test. (F) Statistical comparison of editing efficiencies between WT SaCas9 and the KRH variant across different PAM classes (NNARRT, NNCRRT, NNTRRT, and NNGRRT). Data are shown as mean \pm s.d.; statistical significance was assessed using a two-tailed unpaired Student's t -test.

In HEK293T cells, KRH-ABE exhibited substantially higher base-editing efficiencies than WT-ABE at all tested loci, including those with classical NNGRRT PAMs (Figure 3A). At the *EMX1* locus, the A11 editing efficiency increased from 14.5% with WT-ABE to 81.1% with KRH-ABE, representing a 5.6-fold enhancement; at the *RUNX1* locus, the A15 editing efficiency increased from 0.3% with WT-ABE to 19.5% with KRH-ABE, representing a 65-fold enhancement. In A549, HeLa, and U2OS cells, KRH-ABE again showed consistently higher editing efficiency at non-classical PAM sites, while maintaining comparable activity to WT-ABE at classical PAM targets (Figure 3B–D). These results demonstrate that KRH-ABE can target a wider set of genomic sites than the WT SaCas9-based editor.

As observed with genome editing, ABE performance varied across cell types (Figure 3A–D), but KRH-ABE consistently outperformed WT-ABE at non-classical PAM loci in every cell line tested. On average, KRH-ABE increased editing efficiency by 9.4-fold in HEK293T cells, 3.5-fold in A549 cells, 4.6-fold in HeLa cells, and 6.3-fold in U2OS cells (Figure 3E).

We also compared performance across PAM categories (Figure 3F). KRH-ABE improved editing efficiency by an average of 6.5-fold at NNARRT PAM sites, 4.7-fold at NNCRRRT sites, and 6.5-fold at NNTRRT sites. At canonical NNGRRT PAMs, KRH-ABE displayed slightly higher (but overall comparable) efficiency relative to WT-ABE.

Finally, we assessed potential off-target (OT) effects. KRH-ABE showed OT edits at rates comparable to WT-ABE, indicating that the KRH variant maintains the low OT activity characteristic of WT SaCas9 (Figure S2). Collectively, these results show that KRH-ABE substantially broadens the targeting range of SaCas9-based base editors while preserving high specificity, thereby experimentally validating the computational predictions underlying the KRH design.

KRH SaCas9 demonstrates editing efficiency comparable to KKH SaCas9

The previously reported KKH variant also relaxes the PAM preference of SaCas9, enabling recognition of the same NNNRRT PAM motif (Kleinstiver et al., 2015). Thus, a direct comparison between KKH and our newly designed KRH variant is conducted. Structurally, both triple mutants share two key features: in each, the E782K mutation forms a favorable salt bridge with the backbone phosphate of non-target strand (NTS) nucleotide 9 (e.g. DG9*), and the R1015H mutation is stabilized by Glu993 through an oriented hydrogen bond (Figure 4A). The only structural differences arise at residue 968. In KKH, the N968K substitution forms a single salt bridge with the phosphate of target strand (TS) nucleotide 2 (e.g., DT2), whereas in KRH, the N968R substitution forms two salt bridges with the phosphate groups of TS nucleotides 2 and 3 (e.g., DT2 and DA3) (Figure 4A).

To directly compare their activities, we evaluated the editing efficiencies of KKH and KRH across multiple genomic loci bearing different PAM sequences. At all tested sites, KRH exhibited editing efficiencies comparable to those of KKH (Figure 4B). Overall, both variants displayed similar performance, without systematic advantages for either enzyme (Figure 4C).

We also compared base-editing activities of ABE systems constructed from each variant (KKH-ABE vs. KRH-ABE). Consistent with the genome-editing results, the two base editors showed comparable efficiencies across all tested PAM contexts (Figure 4D,E).

Discussion

In this study, we demonstrate that a fully computational protein design strategy based on UniDesign can generate SaCas9 variants with relaxed PAM specificity and high genome-editing activity. The KRH variant matches the performance of the evolution-derived KKH, establishing UniDesign as a predictive framework for PAM engineering rather than a descriptive or post hoc tool. Moreover, this study highlights that UniDesign enables rapid and scalable exploration of sequence space without requiring iterative experimental screening, offering a complementary—and potentially more efficient—alternative to directed evolution for future protein engineering applications.

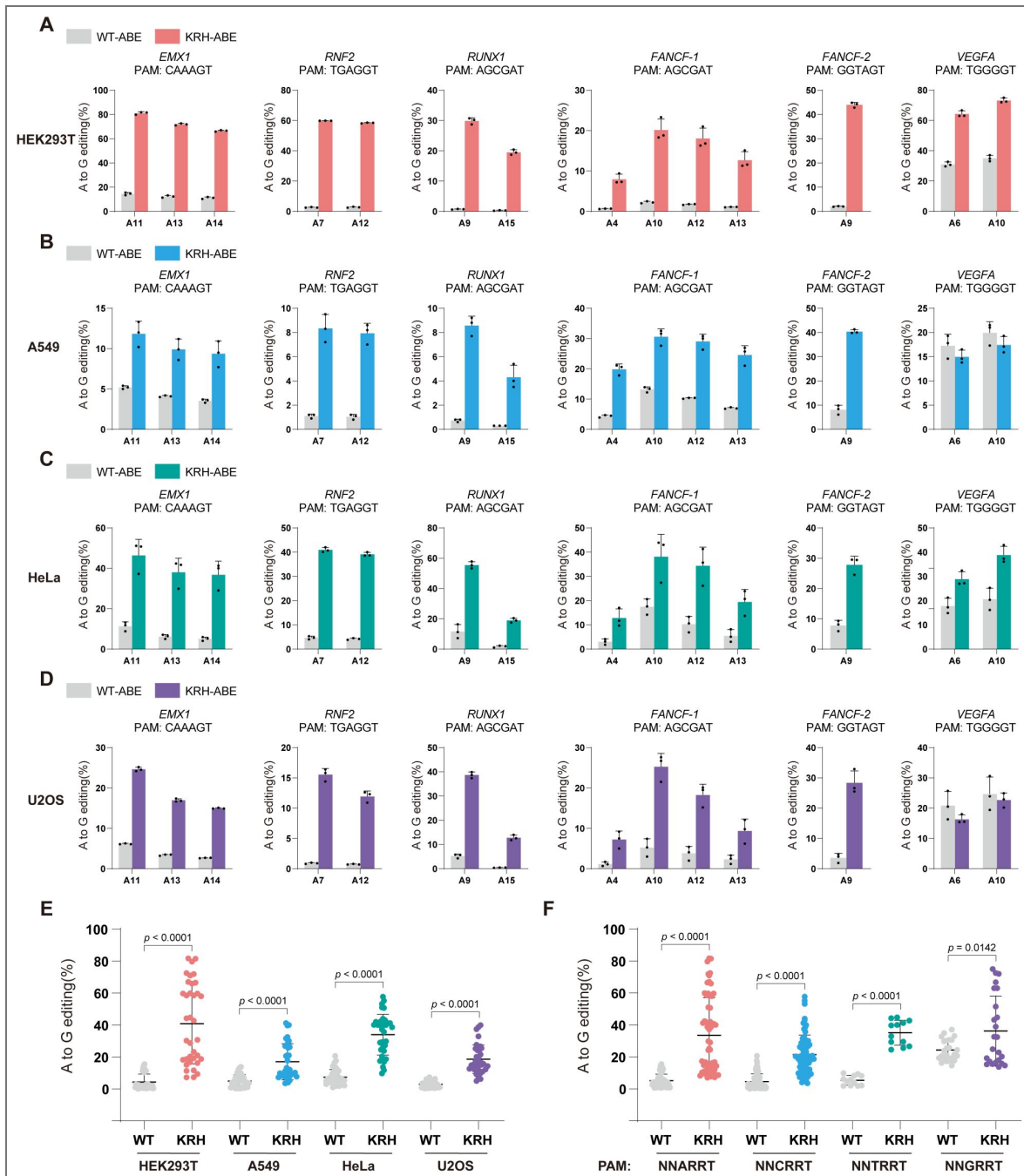


Figure 3. KRH-based ABE further broadens base-editing capabilities.

(A) Base-editing efficiencies of WT-ABE and KRH-ABE at different PAM sites in HEK293T cells. Bars represent the mean of $n = 3$ independent biological replicates; error bars indicate s.d. (B) Base-editing efficiencies of WT-ABE and KRH-ABE at different PAM sites in A549 cells. Bars represent the mean of $n = 3$ independent biological replicates; error bars indicate s.d. (C) Base-editing efficiencies of WT-ABE and KRH-ABE at different PAM sites in HeLa cells. Bars represent the mean of $n = 3$ independent biological replicates; error bars indicate s.d. (D) Base-editing efficiencies of WT-ABE and KRH-ABE at different PAM sites in U2OS cells. Bars represent the mean of $n = 3$ independent biological replicates; error bars indicate s.d. (E) Statistical comparison of base-editing efficiencies between WT-ABE and KRH-ABE at non-canonical PAM sites across HEK293T, A549, HeLa, and U2OS cells. Data are shown as mean \pm s.d.; statistical significance was assessed using a two-tailed unpaired Student's t -test. (F) Statistical comparison of base-editing efficiencies between WT-ABE and KRH-ABE across different PAM classes (NNARRT, NNCRRT, NNTRRT, and NNGRRT). Data are shown as mean \pm s.d.; statistical significance was assessed using a two-tailed unpaired Student's t -test.

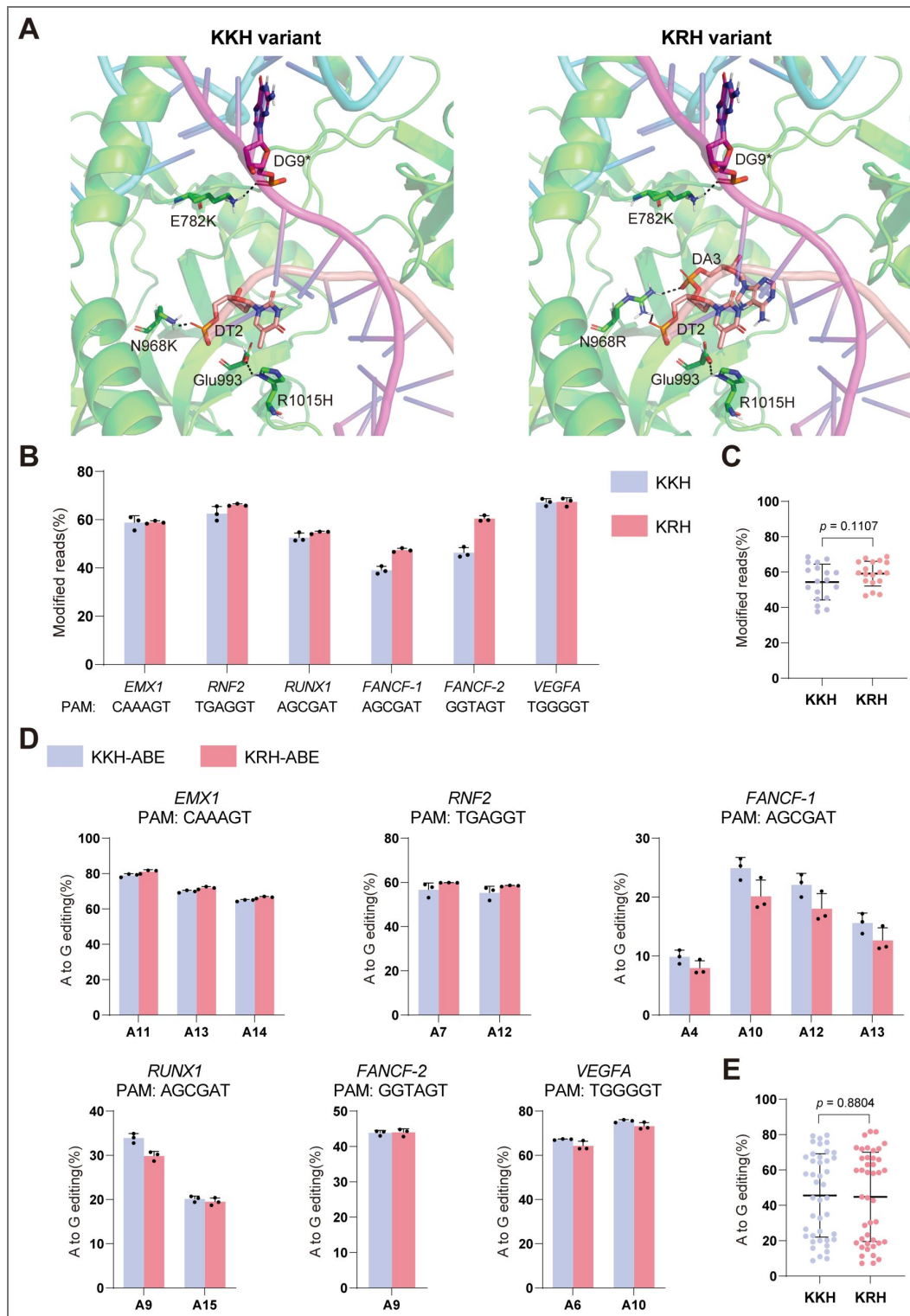


Figure 4. Comparison of KKH and KRH *Staphylococcus aureus* Cas9 variants.

(A) UniDesign models of the KKH and KRH variants. Non-target strand (NTS) nucleotides are indicated by asterisks. (B) Editing efficiencies of the KKH and KRH variants at different PAM sites in HEK293T cells. Bars represent the mean of $n = 3$ independent biological replicates; error bars indicate s.d. (C) Statistical comparison of editing efficiencies between the KKH and KRH variants in HEK293T cells. Data are shown as mean \pm s.d.; statistical significance was assessed using a two-tailed unpaired Student's t -test. (D) Base-editing efficiencies of KKH-ABE and KRH-ABE in HEK293T cells. Bars represent the mean of $n = 3$ independent biological replicates; error bars indicate s.d. (E) Statistical comparison of base-editing efficiencies between KKH-ABE and KRH-ABE in HEK293T cells. Data are shown as mean \pm s.d.; statistical significance was assessed using a two-tailed unpaired Student's t -test.

Mechanistically, our results indicate that PAM recognition and editing activity are governed by a balance between sequence-specific interactions with PAM bases and nonspecific interactions with the DNA backbone. Fine-tuning this balance of specificity and nonspecificity provides a rational strategy for engineering Cas9 variants with relaxed PAM requirements. UniDesign modeling revealed that WT SaCas9 exhibits a strong binding preference for the canonical TTGGGT PAM relative to alternative PAMs (TTAGGT, TTCGGT, and TTTGGT), and that Arg1015 is a key molecular determinant mediating specific recognition of the guanine at the third PAM position. Disrupting this specific interaction by substituting Arg1015 with His substantially reduced SaCas9 activity toward the TTGGGT PAM, whereas the R1015A mutation nearly abolished editing activity altogether (Kleistiver et al., 2015). These effects are consistent with UniDesign predictions, which indicate a marked reduction in binding interactions upon disruption of the Arg1015–guanine hydrogen-bonding interactions (Figure 1E; Data S1). Together, these observations indicate that excessively weakened binding to the native PAM is insufficient to support robust editing. Consequently, enhancing nonspecific Cas9–DNA interactions emerges as a natural and effective strategy to restore activity while preserving equivalent recognition of relaxed PAMs at the third PAM position. Through iterative, fully computational design, we identified triple mutants with mean binding energies comparable to that of WT SaCas9 on the native TTGGGT PAM, a prediction that was fully supported by subsequent experimental validation.

Compared with prior approaches, our method is distinguished by its fully computation-driven nature and minimal reliance on empirical screening or expert heuristics. While previous studies achieved effective PAM relaxation, they typically required extensive wet-lab evolution and/or computationally expensive simulations. In contrast, the improved UniDesign workflow enables efficient and direct exploration of promising point mutations. Depending on the number of design sites, variants generated, and stages of iterative design, a single UniDesign run on one PAM model (e.g. TTAGGT) can be completed in minutes to several hours, making our approach well suited for rapid and scalable Cas9 variant discovery.

While the KRH variant differs from the experimentally evolved KKH by only a single residue, to the best of our knowledge, the N968R mutation has not been experimentally characterized prior to this study and was identified through our computational design workflow. From a practical perspective, although the KKH variant exhibits robust editing activity comparable to that of KRH, we consistently observed higher editing efficiencies for KRH at a subset of target sites (Figure 4B). This site-dependent advantage suggests that KRH may achieve a more favorable balance between PAM flexibility and target DNA engagement, potentially resulting in enhanced catalytic efficiency under certain sequence or chromatin contexts. Accordingly, KRH represents a compelling alternative to KKH in applications where maximal editing efficiency is required, particularly for targets that are suboptimal or only weakly accessible to existing SaCas9 variants. More broadly, these results demonstrate that computationally designed variants can not only recapitulate but, in some cases, surpass the performance of evolution-derived nucleases.

Finally, we emphasize that SaCas9 holds significant therapeutic potential for CRISPR-based disease applications due to its compact size, which enables packaging into a single AAV vector. The development of the KRH variant expands both the targeting range and efficiency of SaCas9, representing an important advance that may reduce reliance on dual-AAV split-Cas9 delivery strategies, which are often associated with lower efficiency (Chew et al., 2016; Moreno et al., 2018).

This study has several limitations. First, our computational design relies on the availability of high-quality Cas9 structures in complex with target DNA. Although high-resolution experimental structures exist for extensively studied enzymes such as SpCas9 (Anders et al., 2014; Jinek et al., 2014; Nishimasu et al., 2014) and SaCas9, they are not always available for other Cas proteins of interest. This limitation may be partially mitigated by advances in deep learning-based structure prediction methods, such as AlphaFold3 (Abramson et al., 2024), which can generate high-quality models of protein–DNA complexes. Second, although KRH exhibited high editing efficiency at both canonical and relaxed PAMs in HEK293T cells (approximately 50–70% modified reads; Figure 2A), substantially lower activity was observed at the tested sites in other cell types,

particularly in A549 cells (approximately 4–20% modified reads; [Figure 2B](#)). This cell-type dependence likely reflects differences in chromatin accessibility and/or the expression levels of key DNA repair pathway components. Further engineering of SaCas9 to enhance activity in such “hard-to-edit” cellular contexts will be an important direction for future work.

Looking forward, the UniDesign framework and design strategy presented here can be extended to other Cas enzymes, providing a general approach for engineering CRISPR enzymes toward diverse functional goals. For instance, we are currently assessing the applicability of this strategy to the design of PAM-relaxed Cas8 variants. Moreover, recent work by Shi et al. revealed a two-step target capture mechanism for efficient CRISPR–Cas9 editing, in which highly PAM-relaxed Cas9 variants like SpRY can become kinetically trapped between steps, reducing overall editing efficiency ([Shi et al., 2025](#)). This suggests that, rather than relying on a single broadly PAM-compatible Cas9, a catalog of Cas9 variants—each optimized for a subset of PAM sequences with high specificity—may represent a more effective strategy for high-efficiency, high-fidelity genome editing ([Collias and Beisel, 2021](#)). We anticipate that UniDesign and continued methodological improvements will facilitate the rational development of such Cas9 catalogs for next-generation genome editing applications.

Methods

SaCas9 structure preprocessing and PAM variant generation

The crystal structure of SaCas9 bound to sgRNA and target DNA (PDB: 5AXW; PAM: TTGGGT) was downloaded from the Protein Data Bank and processed as previously described ([Huang et al., 2023b](#)). Specifically, UniDesign’s *RepairStructure* and *Minimization* modules were applied to add missing side-chain atoms and optimize side-chain conformations to reduce steric clashes.

To evaluate our computational approach for relaxing PAM specificity, we focused on the most strictly required nucleotide within the SaCas9 PAM—the guanine at the third position of NNGRRT. Using the preprocessed 5AXW structure as a template, we used UniDesign’s *BuildMutant* function to generate four structural models differing only in the PAM and its base-paired positions: TTAGGT, TTCGGT, TTGGGT, and TTTGGT. These variants enabled systematic assessment of sequence-dependent structural changes introduced by alternative nucleotides at the critical PAM position.

Design sites selection

Protein design sites were classified into two categories: mutable and repackable. Mutable sites are residues allowed to change amino-acid identity during design. Repackable sites are neighboring residues whose side-chain conformations may be adjusted to accommodate mutations at mutable sites; these residues are not themselves mutated. Using the 5AXW structure visualized in PyMOL, we selected mutable and repackable sites according to the following rules.

Mutable sites included: (1) Arg1015, which directly recognizes the third guanine of the PAM; (2) residues with any side-chain atom within 4.5 Å of the side chain of Arg1015; and (3) residues with any side-chain atom within 6 Å of the main-chain atoms of the PAM, its reverse-complement nucleotides, and the nucleotides located three bases upstream and downstream of both the PAM and its reverse complement.

Repackable sites were defined as protein residues whose side-chain atoms lie within 4.5 Å of the side-chain atoms of any mutable site, allowing localized structural relaxation during design.

The final mutable sites were: Lys37, Glu782, Asn785, Asp786, Thr787, Tyr789, Asn803, Lys815, Lys818, Lys822, Tyr882, Asn885, Asn888, Ala889, Ser908, Leu909, Lys910, Pro911, Asn968, Ile982, Leu988, Glu993, Arg1002, Arg1012, Pro1013, Arg1015, and Thr1019.

The final repackable sites were: Ile784, Ile801, Asn804, Leu805, Asn813, Asp814, Leu827, Val905, Leu907, Lys929, Asn930, Arg980, Leu989, Arg991, Asn995, Tyr1001, Asp1010, Pro1014, and Ile1017.

Improvement of UniDesign for designing point-mutation variants

Relative to earlier UniDesign versions (Huang et al., 2023a [↗](#); Huang et al., 2023b [↗](#)), the main enhancement in current version (v1.2) is the introduction of new score terms that allow explicit control over the number of mutations in designed variants. Below, we summarize these updates.

The original UniDesign scoring function is defined as:

$$E_{\text{total}} = E_{\text{UniEF},\text{non-bind}} + w_{\text{UniEF},\text{bind}} E_{\text{UniEF},\text{bind}} + w_{\text{evo}} E_{\text{evo}}$$

Here, $E_{\text{UniEF},\text{non-bind}}$ and $E_{\text{UniEF},\text{bind}}$ are non-binding and binding energies computed using the UniEF energy function. E_{evo} is an evolutionary term used primarily for de novo protein sequence design. The weights w control the relative contributions of each term, and by default both $w_{\text{UniEF},\text{bind}}$ and w_{evo} are set to 1. The evolutionary term is optional and typically disabled in protein redesign tasks.

To bias the design process toward generating variants with a specific number of point mutations, two additional penalty terms were introduced. The updated scoring function is:

$$E_{\text{total}} = E_{\text{UniEF},\text{non-bind}} + w_{\text{UniEF},\text{bind}} E_{\text{UniEF},\text{bind}} + w_{\text{evo}} E_{\text{evo}} + w_{\text{OOR}} N_{\text{OOR}} + w_{\text{exist}} X_{\text{exist}}$$

The first three terms match the original score function. The newly added terms are:

1. Mutation-count penalty ($w_{\text{OOR}} N_{\text{OOR}}$)

This term penalizes designs whose total number of mutations (n_{mut}) falls outside the user-specified mutation-count range $[N_{\text{mut},\text{min}}, N_{\text{mut},\text{max}}]$:

$$N_{\text{OOR}} = \begin{cases} N_{\text{mut},\text{min}} - n_{\text{mut}}, & \text{if } n_{\text{mut}} < N_{\text{mut},\text{min}} \\ n_{\text{mut}} - N_{\text{mut},\text{max}}, & \text{if } n_{\text{mut}} > N_{\text{mut},\text{max}} \\ 0, & \text{otherwise.} \end{cases}$$

This encourages the SAMC search to remain within the desired mutation-count range (e.g., exactly one mutation, or up to two mutations).

2. Duplicate-design penalty ($w_{\text{exist}} X_{\text{exist}}$)

To prevent the same low-energy variant from being repeatedly generated across independent SAMC trajectories, designs that match a previously saved sequence are penalized:

$$X_{\text{exist}} = \begin{cases} 1, & \text{if the design has already been saved} \\ 0, & \text{otherwise.} \end{cases}$$

This promotes exploration of diverse sequence space.

Both weights w_{OOR} and w_{exist} are set to large positive constants (1000 by default and in this study) to strongly enforce adherence to mutation-count constraints and uniqueness.

In implementation, we did not remove or modify the original UniDesign functionalities for de novo sequence design or applications that do not restrict the number of mutations. Instead, we introduced new optional parameters that allow users to control the mutant-design strategy when desired. Specifically, the options `--min_muts`, `--max_muts`, and `--penalize_identical_seqs` enables users to specify the allowable mutant-count range and to penalize the generation of duplicate sequences. When these options are not used, UniDesign behaves identically to previous versions.

Computational mutant design with improved UniDesign

All computational protein design simulations were performed using UniDesign v1.2. For each design iteration, the input structural model was the preprocessed SaCas9–sgRNA–DNA complex derived from 5AXW, as described above. Design-site constraints were specified using UniDesign’s RESFILE format (Huang et al., 2023a [↗](#); Huang et al., 2023b [↗](#)), and design simulations were performed using the SAMC protocol with mutation-count constraints and duplicate-design

penalties enabled. SAMC trajectories were run using the default UniDesign temperature schedule. Unless otherwise stated, each design iteration generated up to 1000 SAMC trajectories (variants) and was repeated independently 10 times. Among the 10 repeats, the three with the lowest total energy for each PAM model and SaCas9 variant were used for energetic analysis to assess convergence.

Design iteration 1: Identifying mutations at Arg1015 that relax PAM-position specificity

The first design stage focused on exploring amino-acid substitutions at Arg1015, the residue that directly recognizes the third guanine in the NNGRRT PAM. To limit the search to chemically plausible alternatives and avoid destabilizing mutations, we allowed only polar or positively charged amino-acid types at position 1015: {Cys, His, Lys, Asn, Gln, Ser, Thr, Tyr, and the native Arg}. All other mutable residues were fixed to their native identities. These constraints were encoded in a RESFILE, whose content is shown in [Figure S3A](#).

To ensure that at most single-mutation variants were produced, the minimum and maximum allowed mutation counts were set to 0 and 1, respectively. Because position 1015 had only nine allowed amino-acid identities, at most nine unique variants were generated, even though the maximum number of trajectories was set to 1000. Candidate substitutions were evaluated based on total energy, binding energy across four PAM models, and structural inspection for steric compatibility. This stage identified R1015H as the most promising mutation for reducing PAM-position bias.

Design iteration 2: Designing double mutants with R1015H as a fixed background

The second design stage aimed to identify additional mutations that, when combined with R1015H, improved while balancing the mean binding energy across all four modeled PAM variants (TTAGGT, TTCGGT, TTGGGT, and TTTGGT). To accomplish this, residue 1015 was fixed to His, while all other mutable sites were allowed to sample all 20 amino-acid types. The RESFILE content for this iteration is provided in [Figure S3B](#).

The minimum and maximum allowed mutation counts were both set to 2 in this iteration. Each SAMC trajectory generated one unique low-energy double mutant, enforced by sequence-uniqueness constraints. After pooling results across independent runs, candidate double mutants were ranked based on (1) mean binding energy across all four PAM models, (2) structural plausibility, assessed by eliminating variants with steric clashes or unrealistic side-chain orientations, and (3) consistency, assessed by the recurrence of the same mutation across multiple independent SAMC trajectories. Promising second-site mutations identified in this stage included: N968R/K, E782K, T787W/F/M, N803K/W, Y882R, K37R, and K822R.

Design iteration 3: Combining promising mutations into higher-order variants

The third design stage sought to combine the beneficial second-site mutations identified in design iteration 2 into higher-order variants. To restrict the combinatorial space while enriching for functional combinations, each promising position was allowed to sample only the favorable amino-acid types identified previously or its native identity. These constraints were encoded in the RESFILE as follows: Lys37 → {Lys, Arg}; Glu782 → {Glu, Lys}; Thr787 → {Thr, Met, Phe, Trp}; Asn803 → {Asn, Lys, Trp}; Lys822 → {Lys, Arg}; Tyr882 → {Tyr, Arg}; and Asn968 → {Asn, Lys, Arg}. All other mutable sites were fixed to their native identities, and residue 1015 was kept as His for all designs. The RESFILE content for this iteration is provided in [Figure S3C](#).

The minimum and maximum allowed mutation counts were both set to 3 in this iteration. SAMC runs were repeated using the same conditions as above, and variants that consistently emerged across independent runs and exhibited favorable energy profiles were analyzed and selected for experimental characterization.

Plasmids construction

The KKH SaCas9 plasmid was obtained from Addgene (Plasmid #70708). Based on this plasmid, the WT and KRH variants were generated by GenScript. WT-, KKH-, and KRH-based ABE constructs were also synthesized by GenScript. The sequences of all constructs are provided in [Table S1](#).

Each sgRNA expression cassette was synthesized and subsequently cloned into the pUC-GW-Amp vector (Genewiz). The sequences of all sgRNAs used in this study are listed in [Table S2](#).

Cell culture, transfection, and genomic DNA isolation

HEK293T (ATCC, CRL-11268) and A549 (ATCC, CCL-185) cells were cultured in Dulbecco's Modified Eagle Medium (Gibco) supplemented with 10% FBS (Gibco) and 1% penicillin-streptomycin (Gibco). HeLa (ATCC, CCL-2) cells were maintained in Eagle's Minimum Essential Medium (ATCC) supplemented with 10% FBS (Gibco) and 1% penicillin-streptomycin (Gibco). U2OS (ATCC, HTB-96) cells were maintained in McCoy's 5A Medium (ATCC) supplemented with 10% FBS (Gibco) and 1% penicillin-streptomycin (Gibco). All cells were cultured at 37 °C with 5% CO₂ and regularly tested to confirm the absence of mycoplasma contamination. For transfection, cells were seeded into 96-well plates and transfected at approximately 80% confluence with a total of 225 ng plasmid per well (150 ng SaCas9 or ABE plasmid + 75 ng sgRNA plasmid) using JetPRIME (PolyPlus) following the manufacturer's instructions.

Genomic DNA was isolated 72 hours post-transfection using QuickExtractTM DNA Extraction Solution (Lucigen) following the manufacturer's instructions.

Deep sequencing and data analysis

Cell lysates was subjected to PCR amplification of the target loci using specific primers ([Table S3](#)) with barcodes. PCR was performed using the KAPA HiFi PCR Kit (Roche). Equal amounts of PCR products were pooled, purified, and commercially sequenced (Genewiz) using the NovaSeq platform.

Raw FASTQ reads were demultiplexed using bcl2fastq (Illumina) and analyzed using CRISPResso2 (Clement et al., 2019) by aligning amplicon reads to the reference sequences.

Off-target (OT) effect analysis

Potential OT sites (OTS) were predicted using Cas-OFFinder (Bae et al., 2014). The OTS information is provided in [Table S4](#). Predicted OTS regions were amplified by PCR using primers listed in [Table S3](#), followed by deep sequencing. The resulting reads were analyzed to quantify any OT events involving base modifications.

Statistical analysis and reproducibility

All experiments included at least three biological replicates. Data are presented as mean ± s.d. Statistical analyses were performed using GraphPad Prism 9. For two-group comparisons, statistical significance was evaluated using a two-tailed unpaired Student's *t*-test.

Supplementary Information

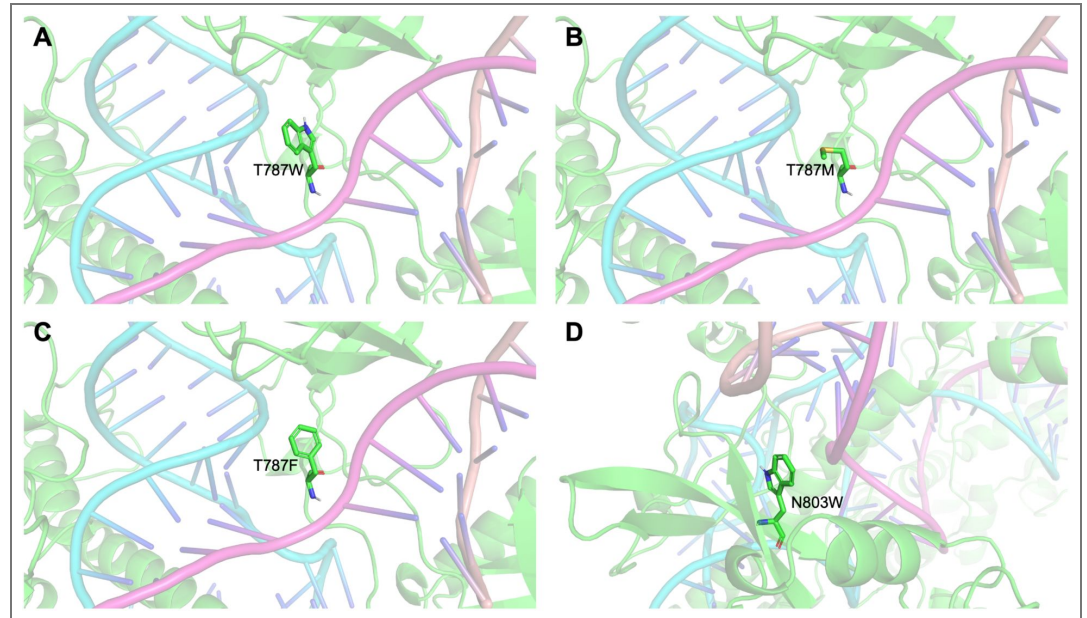


Figure S1. UniDesign models of mutations introducing bulky hydrophobic interactions with the DNA backbone. (A) T787W. (B) T787M. (C) T787F. (D) N803W.

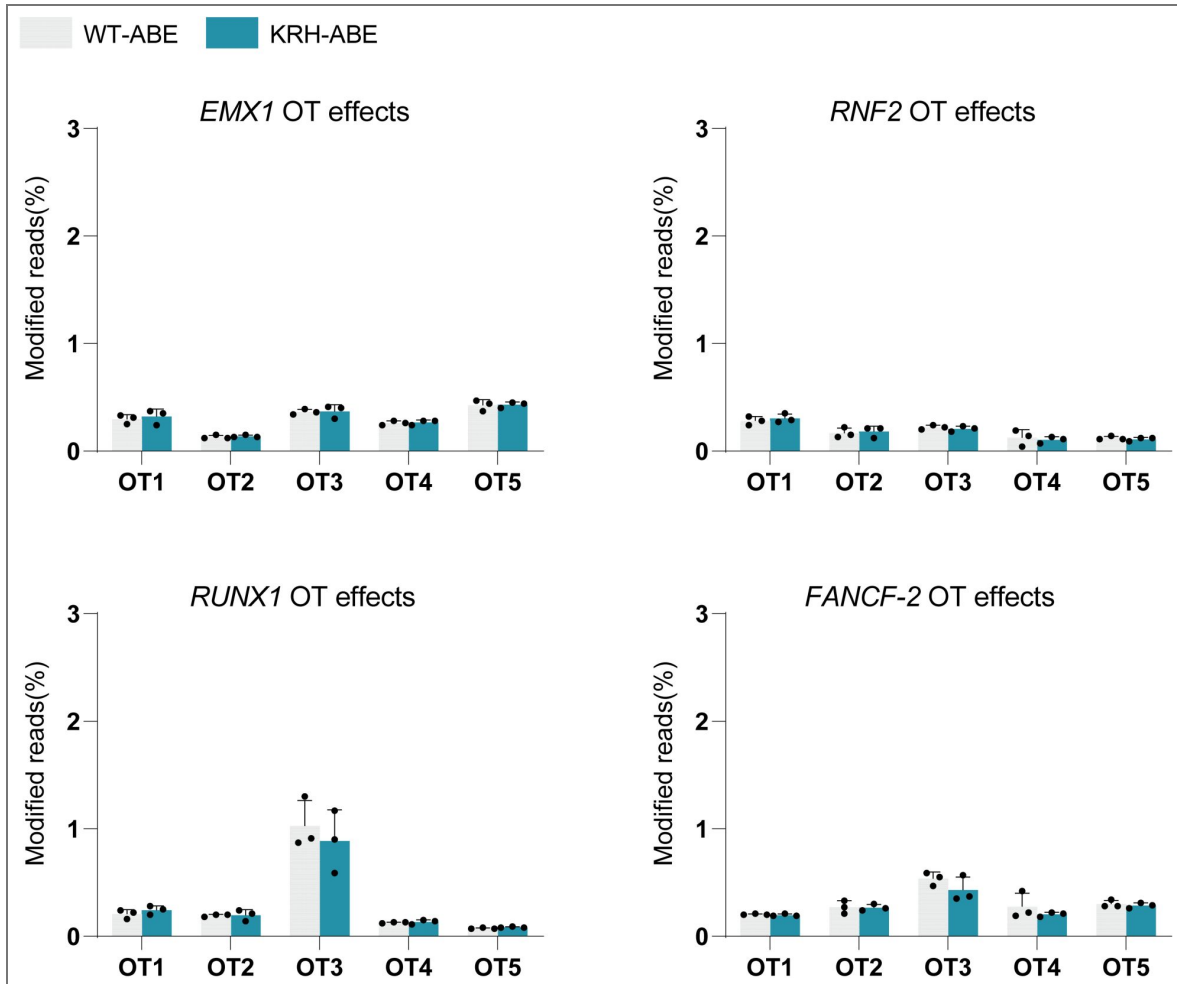


Figure S2. Evaluation of off-target (OT) effects of WT-ABE and KRH-ABE at predicted OT sites.

Bars represent the mean of n = 3 independent biological replicates; error bars indicate s.d.

A			B			C		
SITES_DESIGN_START			SITES_DESIGN_START			SITES_DESIGN_START		
A	37	K # K	A	37	ACDEFGHIKLMNPQRSTVWY # K	A	37	KR # K
A	782	E # E	A	782	ACDEFGHIKLMNPQRSTVWY # E	A	782	EK # E
A	785	N # N	A	785	ACDEFGHIKLMNPQRSTVWY # N	A	785	N # N
A	786	D # D	A	786	ACDEFGHIKLMNPQRSTVWY # D	A	786	D # D
A	787	T # T	A	787	ACDEFGHIKLMNPQRSTVWY # T	A	787	TFMW # T
A	789	Y # Y	A	789	ACDEFGHIKLMNPQRSTVWY # Y	A	789	Y # Y
A	803	N # N	A	803	ACDEFGHIKLMNPQRSTVWY # N	A	803	KNW # N
A	815	K # K	A	815	ACDEFGHIKLMNPQRSTVWY # K	A	815	K # K
A	818	K # K	A	818	ACDEFGHIKLMNPQRSTVWY # K	A	818	K # K
A	822	K # K	A	822	ACDEFGHIKLMNPQRSTVWY # K	A	822	KR # K
A	882	Y # Y	A	882	ACDEFGHIKLMNPQRSTVWY # Y	A	882	YR # Y
A	885	N # N	A	885	ACDEFGHIKLMNPQRSTVWY # N	A	885	N # N
A	888	N # N	A	888	ACDEFGHIKLMNPQRSTVWY # N	A	888	N # N
A	889	A # A	A	889	ACDEFGHIKLMNPQRSTVWY # A	A	889	A # A
A	908	S # S	A	908	ACDEFGHIKLMNPQRSTVWY # S	A	908	S # S
A	909	L # L	A	909	ACDEFGHIKLMNPQRSTVWY # L	A	909	L # L
A	910	K # K	A	910	ACDEFGHIKLMNPQRSTVWY # K	A	910	K # K
A	911	P # P	A	911	ACDEFGHIKLMNPQRSTVWY # P	A	911	P # P
A	968	N # N	A	968	ACDEFGHIKLMNPQRSTVWY # N	A	968	KNR # N
A	982	I # I	A	982	ACDEFGHIKLMNPQRSTVWY # I	A	982	I # I
A	988	L # L	A	988	ACDEFGHIKLMNPQRSTVWY # L	A	988	L # L
A	993	E # E	A	993	ACDEFGHIKLMNPQRSTVWY # E	A	993	E # E
A	1002	R # R	A	1002	ACDEFGHIKLMNPQRSTVWY # R	A	1002	R # R
A	1012	R # R	A	1012	ACDEFGHIKLMNPQRSTVWY # R	A	1012	R # R
A	1013	P # P	A	1013	ACDEFGHIKLMNPQRSTVWY # P	A	1013	P # P
A	1015	CHKNQRSTY # R	A	1015	H # R	A	1015	H # R
A	1019	T # T	A	1019	ACDEFGHIKLMNPQRSTVWY # T	A	1019	T # T
SITES_DESIGN_END			SITES_DESIGN_END			SITES_DESIGN_END		
SITES_REPACK_START			SITES_REPACK_START			SITES_REPACK_START		
A	784	# I	A	784	# I	A	784	# I
A	801	# I	A	801	# I	A	801	# I
A	804	# N	A	804	# N	A	804	# N
A	805	# L	A	805	# L	A	805	# L
A	813	# N	A	813	# N	A	813	# N
A	814	# D	A	814	# D	A	814	# D
A	827	# L	A	827	# L	A	827	# L
A	905	# V	A	905	# V	A	905	# V
A	907	# L	A	907	# L	A	907	# L
A	929	# K	A	929	# K	A	929	# K
A	930	# N	A	930	# N	A	930	# N
A	980	# R	A	980	# R	A	980	# R
A	989	# L	A	989	# L	A	989	# L
A	991	# R	A	991	# R	A	991	# R
A	995	# N	A	995	# N	A	995	# N
A	1001	# Y	A	1001	# Y	A	1001	# Y
A	1010	# D	A	1010	# D	A	1010	# D
A	1014	# P	A	1014	# P	A	1014	# P
A	1017	# I	A	1017	# I	A	1017	# I
SITES_REPACK_END			SITES_REPACK_END			SITES_REPACK_END		

Figure S3. UniDesign RESFILE contents used for SaCas9 redesign.

(A) First iteration. (B) Second iteration. (C) Third iteration.

aggaatggaaaaagctggataaggcaaaagaaagtgatggaaaaaccagatgttcgaggagaagcaggcagagtcaatgcctgagatcgagacagagcagg
 aatacaaggaaatctcatcccctcatcagattaacacataaaggacttcaaagactataatactctcatagggtggacaaaaaaccaatcgcgagct
 cattaatgacacctgtactcaacacggaaggatgataaaggtaataccttgattgtgaataatcttaaggattgatgacaaagataacgacaagctcaaga
 agctgatcaacaagtctccagagaagctccttatgtatcaccacgaccaagactatcagaattgaaactgatcatggagcaatcggggatgagaagaa
 cccactctacaaatattatgaggaaacaggttaattacctgaccaagactccaagaaggataacggaccagtgatcaaaaagataaagtactatggcaacaa
 acttaatgcgcatcttgacataactgacgattacccaattctcgaacaaggttggaagctctccctgaaaccttagatttgactgtacctggataatggg
 gttataaattcgtaccgtgaaaaatctggacgtgatcaaaaaggagaactattatgaagtaaaactaaaagtctatgaggaggcgaagaagctgaagaag
 atctcaatcaggccgagttcatcgcttccttataacaacgatctcatcaagatcaatggagagctttatcgctcattgggtgaaacatgacttctgtaaca
 ggatcgaagtcaatgatagacattacctaccgggagatctcgaacatgaatgataaacggccgctcgaatcatcaagacaatcgatctaaaactca
 gtcaataaaaaagctactctaccgatctcggggaatctctatgaagtgaagtaaaagaagcaccacaaatcattaaaaaaggtggatcccccaagaagaa
 gaggaaagtctcgagcgactacaaagcatgacggtgattataaagatcatgacatcgattacaaggatgacgatgacaagtaaagcggccgactcctca
 ggtgacggctcctatcagaagggtggctggtggtgccaatgccctggctcaaaataccactgagatctttccctctgcaaaaattatggggacatcat
 gaagccccttgagcatctgacttctgctaataaaggaaatctttcattgcaatagtggtggaatctttgtctctactcggaaggacatggggaggg
 caaatcattaaaaatcagaatgagatgtttggttagagtttgccaacatgcccatactgctggctgcatgaacaaaggttggtataaagggtcatcagt
 atatgaaacagcccctgctgtcattccttattccatagaaaagccttgacttgaggtagattttttatattttgtttgtttttttcttaacatccctaaa
 atttccttcatgtttactagccagatctttcctctctcctgactactccagatcatagctgtccctctctcttatggagatccctcgacctgagcccaagctg
 gcgtaatcatggtcatagctgttctctgtgaaatgttatccgctcacaattccacacacatacgagccggaagcataaagtgtaaagcctgggtgcttaa
 tgagtgagtaactcacattaatgcgttgcgctcactgccgcttccagctgggaaacctgtcgtgccagcggatccgcatctcaattagtcagcaaccatagt
 cccgccctaaactccgccatccgcccctaactccgccagttccgccattctccgccatggctgactaattttttattatgagaggccgaggccgct
 cggcctctgagctattccagaagtagtgaggagcctttttggaggcctaggcctttgcaaaaagcctaactgtttattgacgcttataatggttacaataaagc
 aatagcatcaaaaattcacaataaagcattttttcactgcatctagtgtggtttgtcaaaactcatcaatgtatcttatcatgtctggatccgctgcatatg
 aatcgccaacgcgaggagggcgtttgctgattggcgctctccgctcctcgtcactgactcgtcgtcgtcgtcgtcgtcgtcgtcgtcgtcgtcgtcgtc
 agctcactcaaaaggcgttaatacgggtatccacagaatcaggggataacgcaggaaagaacatgtgagcaaaaggccagcaaaaggccaggaaccgtaaa
 aaggccgctgtgctggtttttccataggtcgcctccctcagcagcatcaaaaatcgacgctcaagtcaagggtggcgaaccgacagactataaa
 gataccaggcgtttcccctggaagctcctcgtcgtcctcgttccgacctccgcttaccggatcctgtccgcttctcctctcgggaagcgtggcgttt
 ctcatagctcacgctgtaggtatctcagttcggtgtaggtcgtctcgaagctgggctgtgctcagcaacccccgttcagcccagcctgctccttatccgg
 taactatgctttagtccaaccggtaagacacgacttatcgccactggcagcagcactggtaacaggattagcagagcgaggtatgtagggcgtgctaca
 gagtcttgaagtgggtgctactacggctacactagaagaacagatattggtatctcgcctctgctgaagccagttacctcggaaaaagagtggtagctct
 gatccggcaacaaaccacgctgtagcgtggtttttttgttgcaagcagcagattacgcgcagaaaaaaggatctcaagaagatcctttgatcttttca
 cgggctgacgctcagtggaacgaaaactcaggttaagggatgttgatgagattatcaaaaaggatctcacctagatccttttaataaaaaatgaagtt
 taaatcaatctaaagtataatgagtaaaactggtctgacagttaccaatgcttaacagtgaggcacctatctcagcgtctgtctattctgctcatcattgct
 ctgactcccctgctgtagataactacgatacgggagggttaccatctggccccagtgctgcaatgataaccgagaccacgctcaccgctcagattatc
 agcaataaccagccagccggaaggcggagcgcagaagtgctcctgcaactttatccgctcctcagctctattaattgttccgggaagctagagtaagta
 gttccaggttaatgattgcaacggtgttccattgctacaggtcgtggtgacgctcgtctgttggatgcttattcagctccggttcccaacgatcaa
 ggaggtatcatgatccccatggttgcaaaaagcggtagctcctcgtcctcagctcgttgcaagtaagttggccgaggttatcactcatggttatg
 gcagcactgcataattcttactgtcatgccatccgtaagatctttctgactggtgagtactcaaccaagtcattctgagaatagtgatcgccgacggag
 ttgctctgcccggcgtcaatacgggataataccgcccacatagcagaacttaaaagtctcatcattggaaaaagcttctcggggcgaaaaactcaaggat
 cttaccgctgttagatccagttcgtgtaaccactcgtgacccaactgatctcagcatctttactttcaccagcgttctgggtgagcaaaaacaggaagg
 caaaatgccgcaaaaagggaataaggcgacacgaaatgtgaatactatactctcttttcaatattatgaagcatttatcagggttattgtctcatga
 cgggatacatattgatgtatttagaaaaataaacaatagggttccgcaacatttcccgaagtgccacctg

>KRH-SaCas9

Table S1. (continued)

acgttaaagtcgaagcataaatgggggattcaccagctttctgaggagaaagtggaagttaagaaggaaacgaaacaaaggatacaagcaccatgctgag
 gatgctttgatcatcgctaacgaggctttatctttaaggaatggaaaaagctggataaggcaaaagagtgatggaaaaccagatgttcgaggagaagcag
 gcagagcaatgcctgagatcgagacagagcaggaatacaaggaattttcatccccctcatcagattaaacacataaaggacttcaaagactataaatact
 ctcataggggtggacaaaaacccaatcgcgagctattaatgacaccctgactcaacacggaaggatgataaaggaataactcttgattgtaataatctta
 ggattgatgacaaagataacgacaagctcaagaagctgatcaacaagctccagagaagctccttatgatcaccacgaccacagacttatcagaaattga
 aactgatcatggagcaatacggggatgagaagaaccactctacaaatattatgaggaaacaggaattacctgaccaagtactccaagaaggataacggac
 cagtgatcaaaaagataaagctatggcaacaaactaatgcgcatggacataactgacgattacccaatttctgaaacaagggttggaagctcctctg
 aagccttatagattgacgtgactggataatggggttataaattcgtcaccgtgaaaaatctggacgtgatcaaaaaggagaactattatgaagtaactca
 aagtgtctatgaggaggcgaagaagctgaagaagatctcaatcaggcggattcatcgctccttctataacaacgatctcatcaagatcaatggagagcttta
 tcgctgattggtgtaacaatgacttctgaacaggatcgaagtcaatatgatagacattacctaccgggagatctcgaacacatgaatgataaacggccgc
 ctgcaatcatcaagacaatcgactctaaaactcagtaaaaaaagtactctaccgatactcggggaatctctatgaagtgaagcaaaagacccccaca
 aatcattaaaaaagggtggatcccccaagaagaagaggaaagtctcgagcactacaaagccatgacggtgattataaagatcatgacatcattacaagga
 tgacgatgacaagtaaacggcgcactcctcaggtgaggctgcctatcagaaggtggctggtggtggccaatgcctggctcacaataaccactgagat
 cttttcctctgcaaaaaattatggggacatcatgaagcccttgagcatctgacttctggctaataaaggaaatatttttcttgcaatagtggttgaatttt
 tgtgtctcactcgggaaggacatatgggaggcaaatcatttaaaacatcagaatgagatattggttagagtttgcaacatagcccatatgctggctgcat
 gaacaaaggttgctataaagaggtcatcagtatatgaaacagccccctgctgctcattcctattccatagaaaagccttgactgaggttagatTTTTTatatt
 ttgtttgtgtattttttcttaacatcctaaaattttcttacatgtttactagccagatttttctcctcctcctgactactccagctatagctgctcctctctt
 atggagatccctcgactcgagcccaagctggcgtaatcatggtcatagctgtttctgtgtgaaattgttatccgctcacaattccacacaacatacagccgg
 aagcataaagtgtaaagcctggggtgcctaagtgagtgactcaactacattaatgctgtgctcactgccgcttccagtcgggaaacctgctgctgagcgc
 gatccgcatctcaatagtcagcaaccatagctccgccctaaactccgccatcccggccctaaactccgccagttccgccattctccgcccatggctgactaa
 tttttttattatgacagggcggaggccctcggcctctgagctattccagaagtagtgaggaggctttttggaggcctaggtctttgcaaaaagcctaactgtt
 tattgagcttataatggttacaataaagcaatagcatcacaatttcacaataaagcattttttcactgacttctagttgtggtttgcaaaactcatcaatgt
 atcttatcatgtctggatccgctgacttaataatcgccaacgcggggagaggcggtttgctattgggctccttccgctcctcctcactgactcgtgctg
 ctggctgctggctgcgccgagcggtatcagctcactcaaaaggcggtataacggttatccacagaatcaggggataacgcaggaaagaacatgtgagcaaa
 aggccagcaaaaggccaggaaccgtaaaaaggccgctgctggcgtttttcataggtccgccccctgacgagcatcaaaaaatcgacgctcaagtca
 gaggtggcgaaacccgacaggaactataaagataaccagcggtttccccctggaagctcctcgtgctcctctgttccgacctgcccctaccggatacctgtc
 cgctttctcctcgggaagcgtggcgtttctcatagctcagctgtaggtatctcagttcggtgtaggtcgttcccaagctgggctgtgtgacgaacccc
 ccgttcagcccagccgctgccttatccggtaactatcgtcttgagccaaccggtaagacacgacttatccactggcagcagccactggtaacaggatta
 gcagagcaggtatgtaggcggtctacagatcttgaagtggcctaactacggctacactagaagaacagatatttggtatctgctcctgctgagcca
 gttacctcggaaaaagagttgtagctctgatccggcaaaacaccaccgctgtagcgggtgtttttgttgaagcagcagattacgcgcagaaaaaa
 aggatctcaagaagatcctttgatctttctacgggctgacgctcagtggaacgaaaaactacgtaagggttttggtcatgagattcaaaaaggatcttc
 acctagatccttttaaatataaagtttaaatcaatctaaagtatatatgagtaaaactggtctgacagttaccaatgcttaatcagtgaggcacctatctc
 agcgtatctgtctatcttctcatagttgcctgactccccgctgtgataactacgatacgggagggttaccatctggccccagtgctgcaatgataccgc
 gagaccacgctcaccggctccagattatcagcaataaacgaccagccggaaggccgagcagaagtggtcctgcaacttatccgctccatccagctc
 attaatgttccgggaagctagagtaagtagtccaggttaaatgttgcgaacgttggccattgctacaggcatcgtggtgtcacgctcgtctgttggat
 ggcttattcagctccggttcccaacgatcaaggcgattatgatccccatgttgtgcaaaaaagcggttagctcctcgtctccgatcgtgtcagaagt
 aagttggccgagttatcactcatggtatggcagcactgcataattctctactgcatccatccgtaagatctttctgactggtgagtagtcaaccaa
 gtattctgagaatagtgatcgccgacaggttctcttccggcgctcaatacgggataataaccgcccacatagcagaacttaaaagtctcatcattgg
 aaaaacttctcggggcgaaaaactcaaggatctaccgctgtgagatccagttcagatgaaccactcgtgacccaactgatcttcagatcttttacttca
 ccagctttctgggtgagcaaaaacaggaaggcaaaatccgcaaaaaagggaataaggcgacaggaatgtgaatactcactcttcttttcaata
 ttattgaagcatttatcagggttattgtctcatgagcggatacatattgaaatgtatttagaaaaataacaaatagggggtccgcacattccccgaaaagt

Table S1. (continued)

ccacctg

>KKH-ABE

ggtcgacattgattattgactagtattataatagtaatacaattacggggtcattagttcatagcccatatatggagttccggttacataacttacggtaaatggccc
 gcctggctgaccgccaacgacccccgccattgacgtcaataatgacgtatgtccatagtaacgcaatagggactttcattgacgtcaatgggtggagta
 ttacggtaaaactgcccacttggcagtagatcaatgtagatcatatgccaagtacccccctattgacgtcaatgacggtaaatggcccgcctggcattatgccca
 gtacatgaccttattgggactttcacttggcagtagatctactgattagtcgctattaccatggctgaggtgagccccacgttctgcttactctccccatctc
 cccccctccccacccccattttgtatttatttttttaattttttgtgtagcagtagggggcgggggggggggggggggcgcgccaggcgggggcgggggcg
 gggcgagggggcgggggcgagggcgaggggtgaggcgagccaatcagagcgcgctccgaaagtctttatggcgagggcgggcgggcg
 cggccctataaaaagcgaagcgcggcgggggagtcgctgtagcgtctgccccgctcccgccgctccgcccgcctccgcccgcctccgcccgcctct
 gactgaccgcttactcccacaggtgagcggggcgggagggcctctcctccgggctgtaattagcgttgggttaaatgacggcttgtttctttctgtggctgct
 gaaagccttgaggggctccgggagggcctttgtgagggggagcggctcgggggggtgctgctgtgtgtgtgctggtgggagcggcgtgaggctccgct
 ctgcccggcggtgtagcgtgtagcggcgggcgggcggggctttgtgctcgcagtgtagcggagggagcggcgggggggcggtgccccggtgtagg
 ggggggctgtaggggaaacaaagcgtgtagcgggggtgtagcgtggtgggggtgtagcgggggggtgtagggcgctgtaggggctgcaacccccctgacc
 cccctcccgagttgtagcagcggcccggcttgggtagcgggctcctgtagggcggtggcgggggctccgctgcccggcggggggggggggggggggggg
 gggtagcggggcgggggcgggggcctcggggcggggaggggctggggggagggggcgggcgggccccggagcggcggggctgtagggcgggcgagcc
 gcagccattgctttatgtaaatcgtgtagagggggcgagggacttctttgtccaaatctgtagcggagccgaaatctgggagggcgccgcccacccccctc
 tagggcgggggcggaagcggtagcggcgccggcaggaagaaatggggggggagggccttctgtagcggcgccgctccctctccctctccagcctc
 ggggctgtagcgggggagcggctgcttgggggggacggggcagggcgggggttggcttctgtagcggcgggcttagagcctctgtaacatgtagt
 tcatgcttctttttctacagctcctgggcaacgtgtaggtattgtgctgctcatattttggcaagaattctgtagcgggtagcggggccggggat
 ccaccgtagcaccatgaaacggagcagccgagcgaagcaggttagcagcacaagaagaagcggaaagtcttaggtgaggtttccacagtagtactgg
 atgagacatgacctgacctggccaaggggacgggatgagagggaggtcctgtagggagccgtgtaggtgtagaacaatagagtagcggcgaggggctg
 gaacagagccatggcctgtagcagcccaacagccatgtagaaattgtagcctgtagcagggcgccgctgtagcagaactacagtagtagcagccac
 cctgtagtagcatttagcctgtagtagtagcggcgccatgtagcacttagtagcggcgctgtaggtttgtagtaggagaaactcaaaaagggcgccg
 caggctccctgtagcagtagtagcagcagccggcagcagccgtagcagcagcagcagcagcagcagcagcagcagcagcagcagcagcagcagcagc
 atcggtagcctagacaggttcaatgtagcagaagaagccagagcctcaactcggagtagtagcggagggctcctgtagcagcagcagcagcagcagcagc
 aagcagagcggcagc
 acggaattattgattatgagacagcagtagtagtagcagcggggtaggctgtcaaaagggcacaagcgtgaaacaacaggggaagcagcagcagcagc
 gagcaagaagactcaagc
 caaccctacgagggcgtagtagaaagggctttccagaagcgtgtagcgaagaggagtagcagcagcagcagcagcagcagcagcagcagcagcagc
 gtaaacgaagtaggagggagcagggcaatgaacttagtagcagaagaacagtagtagtagtagtagtagtagtagtagtagtagtagtagtagtagtag
 gcttagagtag
 agcgtaccatcagc
 ggaaggacatcaaggaatggtagcagtag
 gccctcaatgacctcaaacctgtag
 agaagccgacactaaagcagtag
 ctgaaggtgtagcagtag
 ctagttaggacattcagggagtag
 atctgagcctaaagcaatcaacctatttag
 gatctgtagcagcaaaagaaatcctcaaaccttag
 tcataaaaaaacgtag

Table S1. (continued)

accgccagacaaacgaacgcatagaggaaattataagaacaaccggcaaagagaatgccaagatctgatcgagaaatcaagctgcacgacatgcaaga
 aggcgaagtgcctgtactctctggaagctatcccactcgaagatctgtgaataatccattcaattacgaggtggaccacatcatccctagatccgtaagctttgac
 aattcctcaataacaaagtctggttaaacaggaggaaaattctaaaaagggaaccggacccccgttccagtactctgagctccagtgacagcaagattagct
 acgagactttaagaacatattctgaatctggccaaaggcaaaggcaggatcagcaagaccaagaaggagtacctctcgaagaacgcgacattaacagat
 ttagtgtcagaagatttcatcaaccgaaaccttctgatactcggtagccacgagaggcctgatgaatctcctcaggagctacttccgctcaataatctgg
 acgttaaagcaagagcataaatgggggattcaccagctttctgaggagaaagtggaagttaagaaggaacgaacaaaggatacaagcaccatgctgag
 gatgctttgatcatcgtaacgcggactttatcttaaggaatggaaaaagctggataaggcaagaagtgatggaaaaccagatgttcgaggagaagcag
 gcagagtcaatgcctgagatcgagacagagcaggaatacaaggaaatctcatccccctcatcagattaacacataaaggactcaaagactataaatact
 ctcataggggtggacaaaaacccaatcgcaagctcattaatgacaccctgtactcaacacggaaggatgataaaggaataactcttgattgtgaataatctta
 ggattgtatgacaaagataacgacaagctcaagaagctgatcaacaagctcctcagagaagctcttatgtatcaccacgacccacagacttatcagaaattga
 aactgatcatggagcaatacggggatgagaagaaccactctacaaatattatgaggaaacaggttaattactgaccaagtactccaagaaggataacggac
 cagtgtacaaaagataaagctactatggcaacaaactaatgcgcatcttgacataactgacgattacccaattctcgaacaagggttggaagctctccctg
 aagccttatagatttgacgtgtactctggataatggggttataaattctgaccctgaaaaatctggacgtgatcaaaaaggagaactattatgaagtaactca
 aagtgtatgaggaggcgaagaagctgaagaagatctcaatcaggcggatctcatcgtctctctataagaacgactctcatcaagatcaatggagagcttta
 tcgctcattggtgtgaacaatgacttctgaacggatcgaagtaatatgatagacattacctcgggagatctcgaacatgaatgataaacggccgc
 ctacatcatcaagacaatcgactctaaactcagtaataaaaaagctactctaccgatctcgggaaatctctatgaagtgaagcaagaagcaccaca
 aatcattaaaaaggtggatcccccaagaagaagaggaaagctctcagcagactacaaagcatgacggtgattataaagatcatgacatcgattacaagga
 tgacgatgacaagtaaacggcggcactcctcaggtgaggctgctatcagaagggtggctggtgtggccaatgcctggctcacaataaccactgagat
 cttttccctctgcaaaaattatggggacatcatgaagcccttgagcatctgacttctgctaataaaggaaatcttttcttcaatagtggttggaaatctt
 tgtgtctcactcggaggacatgatggagggcaaatcattaaacatcagaatgagatattggttagagttggcaacatgcccatactgctggctgccat
 gaacaaaggttgctataaagaggtcatcagatatgaacagccccctgctgctcattcttccatagaaaagccttgactgaggttagatctttttatatt
 ttgtttgtgtattttttcttaacatccctaaaatcttctacatgtttactagccagatcttctcctcctcactactcccagtcagctgtccctctctct
 atggagatccctcgactcagcccaagcttggcgtaatcatggtcatagctgttctctgtgaaattgttaccgctcacaattccacacaacatacagccgg
 aagcataaagtgtaagcctggggtgcctaagtagtgagtaactcacattaattgctgtgctcactgccgcttccagtcgggaaacctgctgctccagcg
 gatccgcatctcaatagtcagcaaccatagctcccgccctaaactcccccactccgcccactccgcccagttccgcccattctccgcccattggctgactaa
 tttttttatgatcagagccgaggccgctcggccttgagctattccagaagtagtgaggagctttttggaggcctaggtctttgcaaaaagctaaactgtt
 tattgagcttataatggttacaataaagcaatagcatcacaattccacaataaagcattttttcactgacttctagttgtggtttgtccaaactcatcaatgt
 atcttatcatgtctggatccgctgcattaatgaatcgccaacgcggggagagcggtttgctattggcgctcttccgcttctcgtcactgactcgtcgtcg
 ctggctgcttggctgcgggagcggtatcagctcactcaaaaggcggtataacggttatccacagaatcaggggataacgcaggaagaacatgtgagcaaa
 aggccagcaaaaggccaggaaccgtaaaaggccgctgtgctggtttttccataggctccgccccctgacgagcatcaaaaaatcgacgctcaagtca
 gaggtggcgaaccggacagactataaagataaccaggctttccccctggaagctccctcgtgctcctctgtccgacctgcccgttaccggatacctgtc
 cgctttctcctcgggaagcgtggcgtttctcatagctcagctgtaggtatctcagttcgggtaggtcgttccgctcaagctgggctgtgtcacgaacccc
 ccgttcagcccagcctgccttatccggttaactatcgtcttgatccaaccggtaagacacgacttatcgcactggcagcagccactggttaacaggatta
 gcagagcaggtatgtaggcggtctacagagttctgaagtggtggcctaactacggctacactagaagaacagattttggtatctgcctcgtctgtaagcca
 gttacctcggaaaaagagttgtagctctgatccggcaacaaaccaccgctgtagcggtggtttttgtttgcaagcagcagattacgcgcaaaaaaa
 aggatcacaagaagatcctttgatctttctacggggtctgacgctcagtggaacgaaaactcacgtaaggattttggtcatgagattcaaaaaaggatcttc
 acctagatcctttaaataaaaaatgaagtttaaatcaatctaaagtatatatgagtaaaactggtctgacagttaccaatgcttaatcagtgaggcacctatctc
 agcgtatctgtatcttctgtatcctgactccccctgctgtgataactacgatacgggagggcttaccatctggccccagtgctcaatgataccgc
 gagaccacgctcaccggctccagattatcagcaataaaccagccagccggaaggccgagcagaagtggtcctgcaacttatccgctccatccagctc
 attaatgttccgggaagctagagtaagtagttccaggttaatagtttgcgaactgttggccattgctacaggtatctggtgtcacgctcgtctgttggat
 ggcttattcagctccggttccaacgatcaaggcaggtatcatgatccccatggtgtgcaaaaagcggtagctcctcgtcctccgatcgtgtcagaagt

Table S1. (continued)

aagtggccgagtgattactcatggttatggcagcactgcataattcttactgtcatccatccgtaagatgcttttctgtactggtgagtactcaacaa
 gtcattctgagaatagtgatgcgccgaccgagttgctcttcccggcgtaatacgggataataccgcccacatagcagaacttaaaagtctcatcattgg
 aaaacgttcttcggggcgaaaaactcaaggatctaccgctgttgagatccagttcgatgaacccactctgacccaactgatcttcagcatctttactttca
 ccagcgttctgggtgagcaaaaacaggaagcaaaatgcccgaaaaaagggaataaggcgacacggaaatgtgaatactcatactctctttttcaata
 ttattgaagcatttatcagggttattgtctcatgagcggatacatattgaatgtatttagaaaaataacaaataggggttccgcccacattccccgaaaagtg
 ccactg

>KRH-ABE

ggtcgacattgattgactagtattataatagtaatcaattacggggtcattagttcatagccatataatggagttccgcttacataacttacgtaaatggccc
 gcctggctgacccccacgacccccgccattgacgtcaataatgacgtatgtccatagtaacccaatagggaactttcattgacgtcaatgggtggagta
 ttacggtaaactgcccactggcagtcacatcaagtgtatcatatgccaagtacccccctattgacgtcaatgacggtaaatggcccgcctggcattatgccca
 gtacatgaccttatgggactttcacttggcagtcacatctactgtattagtcacgtctattaccatggctgaggtgagccccacgttctgcttactctccccatctc
 cccccctccccacccccattttgtatttttttttaattttttgtgacgagtgggggcggggggggggggggggggcgccgcccagggcggggcggggcg
 gggcgagggcgggggcggggcgagggcgaggggtgcccggcagccaatcagagcggcgctccgaaagtctttttatggcgagggcgggcgggcg
 cggccctataaaaagcgaagcgcggcgggcgggagtcgctgcgctgcttcccggctcccgcctccgcccgcctcgcgcccggcctcggcctc
 gactgacccgcttaccacaggtgagcggggcgggacggcccttctcctcgggctgtaattagcgttggtttaatgacggctgtttctttctgtggctgct
 gaaagccttgaggggctccgggagggcccttgtgcgggggagcggctcgggggggtgctgctgtgtgtgtgctggggagcggcctgctcggctcgcg
 ctcccggcgctgtgagcgtcggggcggcgggggccttgtgctcgcagtgctgcgaggggagcggcggggggcggtgccccgggtgctg
 ggggggctgagggggaacaaaggctgctgcggggtgtgtgctgggggggtgagcagggggtggtggcgcgtcggctcgggctgcaacccccctgacc
 cccctcccaggttctgagcagggcccggcttccgggtcggggctcctgacggggcgtggcggggctcggctcggggcgggggggtggcggcaggtgg
 ggtgcccggcgggggcggggcggcctcgggcccgggagggctcgggggagggcgggcgggccccggagcggcgggctgtcgaggcggcgagcc
 gcagccattgctttatgtaaatctgagagggcgagggacttcttctcccaaatctgtgaggagccgaaatctgggagggcggcggcaccctccta
 gcggcgcgggggcgaagcgggtgcgccggcaggaagaaatggggcgggagggccttctgctgctgcccggcggccttctcctctccagcctc
 ggggctgctcggggggacggctccttccgggggacggggcagggcgggggtcggcttctgctgctgaccggcggcttagagcctctgtaaccatgt
 tcatgcttcttctttctacagctcctgggcaacgtgctggtattgtgctgctcatattttggcaagaattctgagtgacggataccgggccccgggat
 ccaccggtcaccatgaaacggagcggcagcgaagcaggttcgagtcacaaagaagaagcggaaagtctctgaggtggagttttccacgagtactgg
 atgagacatgccctgaccctggccaaggggacgggatgagagggaggtcctgtgggagccgtgctggtgctgaacaatagagtatcgggcagggctg
 gaacagagccatcgccctgacgacccaacagccatgcccgaattatggcctgagacagggcggcctggtcatgcagaactacagactgattgacccac
 cctgtactgacattcgaccttgcgtgatgtgcccggccatgatccactctagatcggcggcgtggttttggatggaggaactcaaaaagggcggc
 caggctccctgatgaacgtgctgaactacccggcatgaatcaccgctgaaattaccgaggaatcctggcagatgaatgtgcccctgctgtgctgatttct
 atcggatgcttagacaggtttcaatgctcagaagaagcccagagctccatcaactccggagatctagcggaggtcctctggctctgagacactggcac
 aagcagagcggcaacactgaaagcagcggggcagcagcgggggtcagggaagcgaattacattctggggctggccattgggataaccagcgttggct
 acggaattattgattatgagacacgcgatgtgattgacccggggttaggctgttcaagaggccaacgttgaaacaacgaggggaagcggagtaagcgcg
 gagcaagaagactcaagcgcagacggagacatcgattcagaggggtgaaaaagctgctcttgattacaatctcctgaccgatcatagtgagctgagcggat
 caaccctacgagggcggagtgaaagggtttccagaagctgtccgaagaggagtctccggcgttctgacactggccaaacggaggggggttcaaat
 gtaaacgaagtggaggagacagggcaatgaacttagtacgaaagaacagatcagtaggaactctaaggctctcgaagagaaatctgctgctgattgca
 gcttgagagactgaaaaagacggcgaagtacgggatctattaataggttcaagactcagattacgtaaaggaagccaagcagctcctgaaagtaagaa
 agcgtaccatcagctgatcagactcatgatacctacatagatttctgagagacagggagacatactacgagggcccaggggaaggtctccttttgggt
 ggaaggacatcaaggaatggatcagagatgcttatgggacattgtacatattttccggaggagctcaggagcgtcaagtacgctcaaatgccacgtgacaat
 gccctcaatgacctcaaacctgattaccagggagcagagaagcgtggagtactatgaaagttccagattatcagagaatgtgttaagcagaaga
 agaagccgacactaagcagattgcaaaaggaaatcctctgtaatgaggaagatataaggagatacagagtgacaagtagcaggcaagccccgaggttcaacaa

Table S1. (continued)

Table S1. (continued)

acctagatccttttaataaaaaatgaagttttaaatacaatctaaagtatatatgagtaaaactggctgacagttaccaatgcttaatacagtgaggcacctatctc
 agcgatctgtctatttcgttcatccatagttgcctgactccccctgctgtagataactacgatacgggagggttacatctggccccagtgctgcaatgataccgc
 gagaccacgctcaccggctccagattatcagcaataaaaccagccagccggaaggccgagcgcagaagtggctcctgcaactttatccgctccatccagctc
 attaattgttccgggaagctagagtaagtagttcggcagtaatagtttgcaacgttggccattgctacagcatcgtgggtgcacgctcgtctgtttggtat
 ggcttattcagctccggttcccaacgatcaaggcagttacatgatccccatggttgcaaaaaagcggtagctcctcggtcctccgatcgttgcaagaat
 aagttggccgagtggtatcactcatggttatggcagcactgcataattcttactgtcatgccatccgtaagatgcttttctgtgactggtagtactcaaccaa
 gtcattctgagaatagtgatgcgccgaccgagttgctcttggcggcgtcaatacgggataataccgcccacatagcagaactttaaagtgtctcatcattgg
 aaaaacttctcggggcgaaaaactcaaggatctaccgctgttgagatccagttcagatgtaaccactcgtgcacccaactgatcttcagcatctttactttca
 ccagctttctgggtgagcaaaaacaggaaggcaaaatgccgcaaaaagggaataaggcgacacggaaatgtgaatactcatacttctcttttcaata
 ttattgaagcattatcagggttattgtctcatgagcggatacatattgaatgtatttagaaaaataacaaataggggtccgcgacatttcccgaaaagtg
 ccactg

Table S2. List of sgRNA sequences used in this study.

Site	Spacer sequence (5'→3')	Scaffold sequence (5'→3')
<i>EMX1</i>	GTGTGGTTCCAGAACCGGAGGA	gttttagtactctgaaacagaatctactaaaaaaggcaaaatgccgtgtttatctcg tcaactgttggcgaga
<i>RNF2</i>	GCAGTCATCTTAGTCATTACC	gttttagtactctgaaacagaatctactaaaaaaggcaaaatgccgtgtttatctcg tcaactgttggcgaga
<i>RUNX1</i>	GAGGGTGCATTTTCAGGAGGA	gttttagtactctgaaacagaatctactaaaaaaggcaaaatgccgtgtttatctcg tcaactgttggcgaga
<i>FANCF-1</i>	GAGACCGCCAGAAGCTCGGAAA	gttttagtactctgaaacagaatctactaaaaaaggcaaaatgccgtgtttatctcg tcaactgttggcgaga
<i>FANCF-2</i>	GGGGTCCCAGGTGCTGACGTA	gttttagtactctgaaacagaatctactaaaaaaggcaaaatgccgtgtttatctcg tcaactgttggcgaga
<i>VEGFA</i>	GGGTGAGTGAGTGTGTGCGTG	gttttagtactctgaaacagaatctactaaaaaaggcaaaatgccgtgtttatctcg tcaactgttggcgaga

Primer name	Sequence(5'→3')
<i>EMX1</i> -onTarget-DS-F	CAGCTCAGCCTGAGTGTGA
<i>EMX1</i> -onTarget-DS-R	CTCGTGGGTTTGTGGTTGC
<i>RNF2</i> -onTarget-DS-F	GCCAACATACAGAAGTCAGGAA
<i>RNF2</i> -onTarget-DS-R	TCAGGCTGTGCAGACAAACG
<i>RUNX1</i> -onTarget-DS-F	AGATGTAGGGCTAGAGGGGTG
<i>RUNX1</i> -onTarget-DS-R	CACCGAGGCATCTCTGCAC
<i>FANCF-1</i> -onTarget-DS-F	TGCATTTGACCAATAGCATTGC
<i>FANCF-1</i> -onTarget-DS-R	ATGGATGTGGCGCAGGTAG
<i>FANCF-2</i> -onTarget-DS-F	TGCATTTGACCAATAGCATTGC
<i>FANCF-2</i> -onTarget-DS-R	ATGGATGTGGCGCAGGTAG
<i>VEGFA</i> -onTarget-DS-F	CAGTACTAGGGGGCGCT
<i>VEGFA</i> -onTarget-DS-R	GAGCCGTTCCCTCTTTGCTA
<i>EMX1</i> -OT1-DS-F	CCCAGCACCTCTACCAATA
<i>EMX1</i> -OT1-DS-R	CACACATCTGTGGAGGGTCTT
<i>EMX1</i> -OT2-DS-F	ACACGTGGATGTGTCTACAGC
<i>EMX1</i> -OT2-DS-R	TTCTGACCTCAGGTGATCCACC
<i>EMX1</i> -OT3-DS-F	GGGCTCGGGAGAGCAGA
<i>EMX1</i> -OT3-DS-R	CGGTTGTATTCGTCGTCGTC
<i>EMX1</i> -OT4-DS-F	GTCAGACGGGAGTCAGAACC
<i>EMX1</i> -OT4-DS-R	GAGTCTCGGAGCTGCCAC
<i>EMX1</i> -OT5-DS-F	TTGCGCCCCTAGTTTTATTG
<i>EMX1</i> -OT5-DS-R	AGCTTCATGGAGGACACTTC
<i>RNF2</i> -OT1-DS-F	CCCACCCCTTTAATCGTT
<i>RNF2</i> -OT1-DS-R	TACAGGGCCAAGGAAGCATAA
<i>RNF2</i> -OT2-DS-F	CAGTGATTGACAAGTAAGTGCAT
<i>RNF2</i> -OT2-DS-R	ACAGTCAGAATGAGCTTGGCT
<i>RNF2</i> -OT3-DS-F	GAGCAGAGGCCTCAGAAGCA
<i>RNF2</i> -OT3-DS-R	CACAGCCTTGACCTAGACTCCT
<i>RNF2</i> -OT4-DS-F	GCTACCACTATTCACCCAGAAGG
<i>RNF2</i> -OT4-DS-R	GGTGGAGAGGAGAGGACCAG
<i>RNF2</i> -OT5-DS-F	TTGGGGAGACAGTTCTCGAAG

Table S3. List of PCR primers used in this study.

<i>RNF2</i> -OT5-DS-R	TGGAGTGGAAAGCAGAAAACCA
<i>RUNX1</i> -OT1-DS-F	TTCTCACACAAAGCGGGGAG
<i>RUNX1</i> -OT1-DS-R	TCTCTATCAGCTGCATCCGC
<i>RUNX1</i> -OT2-DS-F	AAAGGTGTCTCTCGCATCTCC
<i>RUNX1</i> -OT2-DS-R	AAAGGACTCCCATACAGCCAAG
<i>RUNX1</i> -OT3-DS-F	CACAGCCCTTCGTTCAAGTTAC
<i>RUNX1</i> -OT3-DS-R	GCAAGGCTTGCTTTATGTA
<i>RUNX1</i> -OT4-DS-F	ACACAAAGAGTATGTCAGGCCATC
<i>RUNX1</i> -OT4-DS-R	CCTCAACTGACTTCACAGGCT
<i>RUNX1</i> -OT5-DS-F	TCAGAGAGAAAGAGGGGCTGA
<i>RUNX1</i> -OT5-DS-R	CAACACACTGGTTAGGGGTGA
<i>FANCF</i> -2-OT1-DS-F	GAGGACTCGAAGGGGGTTTCA
<i>FANCF</i> -2-OT1-DS-R	TTCAGGGTGAGGGAGGTTTAC
<i>FANCF</i> -2-OT2-DS-F	TGATGAGGAGCAGATGCCTTTT
<i>FANCF</i> -2-OT2-DS-R	AGGTTGATCCTTCTGCCCTGA
<i>FANCF</i> -2-OT3-DS-F	TCATCACTCAAGATACGGGACC
<i>FANCF</i> -2-OT3-DS-R	TGCAGCAGGCTAAACACCTA
<i>FANCF</i> -2-OT4-DS-F	CCCATAAAGGTGATTCCTAGGA
<i>FANCF</i> -2-OT4-DS-R	GGATGGCATGACATTTCTATCATATGC
<i>FANCF</i> -2-OT5-DS-F	CTTTGGCCCGGGAGTAGTTG
<i>FANCF</i> -2-OT5-DS-R	GGGGATGAGACGTGGTCAAG

Table S3. (continued)

Off-target (OT) site	Sequence (5'→3')
<i>EMX1</i> -OT1	GTTTGGTTCAAGAACCGGAGGGCTAAAT
<i>EMX1</i> -OT2	GTGTGGTCCCTGGACCGGAGGCATCAAT
<i>EMX1</i> -OT3	GTCTGGTTCAGAACCGCCGGACCAAGT
<i>EMX1</i> -OT4	GTGTGGTTCAGAACCGCCGGGCCAAGT
<i>EMX1</i> -OT5	GTGTGGTTCAGAACCGACGGGCTAAGT
<i>RNF2</i> -OT1	ACAGTCACATTAGTCATTAGCCTAAAT
<i>RNF2</i> -OT2	GTTGTATCTTAGTCTTTACCTGAGAT
<i>RNF2</i> -OT3	GAAGTCATTGGAGTCATTACCATAAAT
<i>RNF2</i> -OT4	GGAGTCATCTTTGACCTTACCCTAAAT
<i>RNF2</i> -OT5	GCAGTTATATGAGTCATTACTAAAGGT
<i>RUNX1</i> -OT1	GACGGAGCCTTTTCAGGAGGACTTAAT
<i>RUNX1</i> -OT2	GAGGGAGCCTTTCCAGAAGGAGTTGAT
<i>RUNX1</i> -OT3	GAGGGTGGATTTTCAAGAAGGTCAAAT
<i>RUNX1</i> -OT4	GAGGGAGCATTGCAAGAGAAGGTGGT
<i>RUNX1</i> -OT5	GAAGGTGCTTTTTCCCGAGGAGAGAGT
<i>VEGFA</i> -OT1	GGGGTCCCGGTGCTGGGGCATCAGGT
<i>VEGFA</i> -OT2	GGGGTCCCTGATGAAGACGTATTTGGT
<i>VEGFA</i> -OT3	GGGGTCCGGTTTCTGACGTATCCGGT
<i>VEGFA</i> -OT4	GTGGTCCAGATCCTGATGTAGGTGAT
<i>VEGFA</i> -OT5	GGGATCCAGGTGCTGCGGTTCCAGGT

Table S4. Predicted off-target site sequences.

Data availability

All computational protein design data, including designed models and summaries of energetic analyses, are publicly available at <https://doi.org/10.5281/zenodo.18058217>. The deep-sequencing data will be available on the NCBI Sequence Read Archive (SRA). The plasmid materials are available upon request to the corresponding authors.

Acknowledgements

This work was supported by the National Institutes of Health grants (GM149016 to XH and XX; HL164205 to JX). We thank the Advanced Research Computing (ARC) at the University of Michigan for providing the computational resources and services that supported this research.

Additional information

Code availability

The UniDesign program and associated scripts, along with detailed usage documentation, are publicly available at <https://doi.org/10.5281/zenodo.18058217>.

Author contributions

XH conceived and managed the project. XX, JZhang, YEC, and JX supervised the project. XH performed computational studies. YX conducted wet-lab experiments with efforts from LKT, JZhou, and SC. YX and XH wrote the initial manuscript. XX, JZhang, YEC, JX, and XH edited the manuscript. All authors participated in discussions and agreed with the final paper.

Funding

Funder	Grant reference number	Author
HHS National Institutes of Health (NIH)	GM149016	Xiaofeng Xia Xiaoqiang Huang
HHS National Institutes of Health (NIH)	HL164205	Jie Xu

Author ORCID iDs

Xiaoqiang Huang: <https://orcid.org/0000-0002-1005-848X>

Additional files

[Data S1](#)

[Data S2](#)

[Data S3](#)

References

Abramson J, Adler J, Dunger J, Evans R, Green T, Pritzel A, Ronneberger O, Willmore L, Ballard AJ, Bambrick J, *et al.* (2024) Accurate structure prediction of biomolecular interactions with AlphaFold 3. *Nature* **630**:493-500 <https://doi.org/10.1038/s41586-024-07487-w> | [PubMed](#)

Anders C, Niewoehner O, Duerst A, Jinek M (2014) Structural basis of PAM-dependent target DNA recognition by the Cas9 endonuclease. *Nature* **513**:569-573 <https://doi.org/10.1038/nature13579> | [PubMed](#)

Bae S, Park J, Kim JS (2014) Cas-OFFinder: a fast and versatile algorithm that searches for potential off-target sites of Cas9 RNA-guided endonucleases. *Bioinformatics* **30**:1473-1475 <https://doi.org/10.1093/bioinformatics/btu048> | [PubMed](#)

- Chew WL**, Tabebordbar M, Cheng JK, Mali P, Wu EY, Ng AH, Zhu K, Wagers AJ, Church GM (2016) A multifunctional AAV-CRISPR-Cas9 and its host response. *Nat Methods* **13**:868-874 <https://doi.org/10.1038/nmeth.3993> | [PubMed](#)
- Clement K**, Rees H, Canver MC, Gehrke JM, Farouni R, Hsu JY, Cole MA, Liu DR, Joung JK, Bauer DE, *et al.* (2019) CRISPResso2 provides accurate and rapid genome editing sequence analysis. *Nat Biotechnol* **37**:224-226 <https://doi.org/10.1038/s41587-019-0032-3> | [PubMed](#)
- Collias D**, Beisel CL (2021) CRISPR technologies and the search for the PAM-free nuclease. *Nat Commun* **12**:555 <https://doi.org/10.1038/s41467-020-20633-y> | [PubMed](#)
- Doudna JA**, Charpentier E (2014) The new frontier of genome engineering with CRISPR-Cas9. *Science* **346**:1258096 <https://doi.org/10.1126/science.1258096> | [PubMed](#)
- Hsu PD**, Lander ES, Zhang F (2014) Development and applications of CRISPR-Cas9 for genome engineering. *Cell* **157**:1262-1278 <https://doi.org/10.1016/j.cell.2014.05.010> | [PubMed](#)
- Huang X**, Pearce R, Zhang Y (2020) EvoEF2: accurate and fast energy function for computational protein design. *Bioinformatics* **36**:1135-1142 <https://doi.org/10.1093/bioinformatics/btz740> | [PubMed](#)
- Huang X**, Sun Y, Osawa Y, Chen YE, Zhang H (2023a) Computational redesign of cytochrome P450 CYP102A1 for highly stereoselective omeprazole hydroxylation by UniDesign. *J Biol Chem* **299**:105050 <https://doi.org/10.1016/j.jbc.2023.105050> | [PubMed](#)
- Huang X**, Yang D, Zhang J, Xu J, Chen YE (2022) Recent Advances in Improving Gene-Editing Specificity through CRISPR-Cas9 Nuclease Engineering. *Cells* **11**:2186 <https://doi.org/10.3390/cells11142186> | [PubMed](#)
- Huang X**, Zhou J, Yang D, Zhang J, Xia X, Chen YE, Xu J (2023b) Decoding CRISPR-Cas PAM recognition with UniDesign. *Brief Bioinform* **24**:bbad133 <https://doi.org/10.1093/bib/bbad133> | [PubMed](#)
- Jinek M**, Jiang F, Taylor DW, Sternberg SH, Kaya E, Ma E, Anders C, Hauer M, Zhou K, Lin S, *et al.* (2014) Structures of Cas9 endonucleases reveal RNA-mediated conformational activation. *Science* **343**:1247997 <https://doi.org/10.1126/science.1247997> | [PubMed](#)
- Kleinstiver BP**, Prew MS, Tsai SQ, Nguyen NT, Topkar VV, Zheng Z, Joung JK (2015) Broadening the targeting range of Staphylococcus aureus CRISPR-Cas9 by modifying PAM recognition. *Nat Biotechnol* **33**:1293-1298 <https://doi.org/10.1038/nbt.3404> | [PubMed](#)
- Komor AC**, Badran AH, Liu DR (2017) CRISPR-Based Technologies for the Manipulation of Eukaryotic Genomes. *Cell* **168**:20-36 <https://doi.org/10.1016/j.cell.2016.10.044> | [PubMed](#)
- Luan B**, Xu G, Feng M, Cong L, Zhou R (2019) Combined Computational-Experimental Approach to Explore the Molecular Mechanism of SaCas9 with a Broadened DNA Targeting Range. *J Am Chem Soc* **141**:6545-6552 <https://doi.org/10.1021/jacs.8b13144> | [PubMed](#)
- Ma D**, Xu Z, Zhang Z, Chen X, Zeng X, Zhang Y, Deng T, Ren M, Sun Z, Jiang R, *et al.* (2019) Engineer chimeric Cas9 to expand PAM recognition based on evolutionary information. *Nat Commun* **10**:560 <https://doi.org/10.1038/s41467-019-08395-8> | [PubMed](#)
- Moreno AM**, Fu X, Zhu J, Katrekar D, Shih YV, Marlett J, Cabotaje J, Tat J, Naughton J, Lisowski L, *et al.* (2018) In Situ Gene Therapy via AAV-CRISPR-Cas9-Mediated Targeted Gene Regulation. *Mol Ther* **26**:1818-1827 <https://doi.org/10.1016/j.ymthe.2018.04.017> | [PubMed](#)
- Nishimasu H**, Cong L, Yan WX, Ran FA, Zetsche B, Li Y, Kurabayashi A, Ishitani R, Zhang F, Nureki O (2015) Crystal Structure of Staphylococcus aureus Cas9. *Cell* **162**:1113-1126 <https://doi.org/10.1016/j.cell.2015.08.007> | [PubMed](#)
- Nishimasu H**, Ran FA, Hsu PD, Konermann S, Shehata SI, Dohmae N, Ishitani R, Zhang F, Nureki O (2014) Crystal structure of Cas9 in complex with guide RNA and target DNA. *Cell* **156**:935-949 <https://doi.org/10.1016/j.cell.2014.02.001> | [PubMed](#)
- Ran FA**, Cong L, Yan WX, Scott DA, Gootenberg JS, Kriz AJ, Zetsche B, Shalem O, Wu X, Makarova KS, *et al.* (2015) In vivo genome editing using Staphylococcus aureus Cas9. *Nature* **520**:186-191 <https://doi.org/10.1038/nature14299> | [PubMed](#)

Richter MF, Zhao KT, Eton E, Lapinaite A, Newby GA, Thuronyi BW, Wilson C, Koblan LW, Zeng J, Bauer DE, *et al.* (2020) Phage-assisted evolution of an adenine base editor with improved Cas domain compatibility and activity. *Nat Biotechnol* **38**:883-891 <https://doi.org/10.1038/s41587-020-0453-z> | [PubMed](#)

Shi H, Al-Sayyad N, Wasko KM, Trinidad MI, Doherty EE, Vohra K, Boger RS, Colognori D, Cofsky JC, Skopintsev P, *et al.* (2025) Rapid two-step target capture ensures efficient CRISPR-Cas9-guided genome editing. *Mol Cell* **85**:1730-1742. <https://doi.org/10.1016/j.molcel.2025.03.024> | [PubMed](#)

Sun Y, Huang X, Zhang J, Osawa Y, Chen YE, Zhang H (2026) Computational Design of CYP102A1 Variants for Biosynthesis of a Next-Generation Antiplatelet Drug DT-678. *ACS Synth Biol* **15**:1082-1089 <https://doi.org/10.1021/acssynbio.5c00768> | [PubMed](#)

Huang X (2025) Fully computational design of SaCas9 with relaxed PAM requirement. Zenodo. <https://doi.org/10.5281/zenodo.18058217>

Peer reviews

Reviewer #1 (Public review):

[Editors' note: The Reviewing Editor has assessed the work without involving the previous reviewers, updating the eLife Assessment accordingly. The authors did an excellent job of addressing the reviewers' comments and suggestions. The manuscript is now in line with the minor suggestions from the original reviewers, who were already enthusiastic about the first version.]

Summary:

This manuscript by Xiong and colleagues presents a compelling validation of UniDesign, a fully computational protein design framework, by using it to engineer a novel, PAM-relaxed variant of *Staphylococcus aureus* Cas9 (SaCas9) named KRH. The core achievement is the successful de novo generation of a high-performance nuclease (E782K/N968R/R1015H) solely through in silico modeling, without any subsequent experimental optimization or directed evolution. The authors demonstrate that KRH expands the SaCas9 PAM specificity from NNGRRT to NNNRRT, achieving genome editing and base editing efficiencies across multiple human cell types that are comparable to, and sometimes exceed, the well-known evolution-derived KKH variant. The work positions UniDesign not merely as an analytical tool, but as a powerful engine for the generative design of complex molecular functions, offering a scalable and mechanistically insightful alternative to traditional experimental screening.

Strengths:

This is an outstanding manuscript that serves as a powerful proof-of-concept for the next generation of computational protein design. The primary selling point—the raw predictive and generative power of UniDesign—is convincingly demonstrated throughout.

The manuscript shows that the tool can:

- (1) successfully navigate a complex sequence landscape to identify a minimal set of three mutations (KRH) that remodel a critical protein-DNA interface;
- (2) accurately model and balance the delicate interplay between specific base contacts and non-specific backbone interactions to achieve relaxed PAM specificity;
- (3) deliver a final product whose performance is indistinguishable from, and in some cases superior to, a variant that required extensive wet-lab evolution.

The experimental validation is rigorous, thorough, and directly supports the computational predictions. This work will stand as a landmark study for the field, illustrating that

computational design has matured to the point where it can reliably generate sophisticated tools for genome engineering.

(1) Demonstration of Generative Power:

The most significant finding is that UniDesign, without any experimental feedback, generated a variant (KRH) that matches the performance of the evolution-derived KKH. This is a remarkable achievement. The iterative design strategy—first reducing PAM bias (R1015H), then restoring binding through non-specific interactions (e.g., N968R, E782K)—is a textbook example of rational design, but it is executed entirely by the algorithm. This validates UniDesign's energy function and search algorithm as capable of capturing the subtle biophysical principles governing PAM recognition.

(2) Mechanistic Insight as a Built-in Feature:

A key advantage of UniDesign highlighted by this work is its inherent ability to provide mechanistic explanations. The computational models not only predicted which mutations would work (e.g., N968R over N968K in the KRH variant) but also why they work. The structural and energetic analyses showing the bidentate salt bridge formed by Arg968 versus the single bond formed by Lys968 (Figure 4A) is a perfect example of how the tool's output can rationalize functional differences, a level of insight that is rarely attainable from directed evolution campaigns alone.

(3) Scalability and Accessibility for Engineering:

The authors explicitly contrast UniDesign's efficiency (minutes to hours per design run) with the computational expense of methods like COMET and the experimental overhead of directed evolution. The improvements to UniDesign v1.2, specifically the mutation-count and sequence-uniqueness penalties, directly address a key challenge in computational design (generating diverse, low-energy point-mutant libraries). This positions the tool as a highly accessible and scalable platform for engineering other CRISPR systems, a point that will be of immense interest to the community.

<https://doi.org/10.7554/eLife.110906.2.sa3>

Reviewer #2 (Public review):

Summary:

This manuscript describes the fully in silico design of a new variant of *Staphylococcus aureus* Cas9 (SaCas9) using an improved UniDesign workflow.

The design strategy consists of three sequential steps:

- (1) Reducing positional bias at PAM position 3;
- (2) Restoring DNA binding through nonspecific interactions;
- (3) Combining individually favorable substitutions.

The overall pipeline is conceptually elegant and logically structured, and the genome-editing activity of the designed variants is comprehensively characterized. The resulting KRH variant exhibits relaxed PAM specificity, expanding the targeting range of SaCas9 across diverse cell types. Notably, the KRH variant demonstrates performance comparable to that of the evolution-derived KKH variant, underscoring the effectiveness of the proposed computational design framework.

<https://doi.org/10.7554/eLife.110906.2.sa2>

Reviewer #3 (Public review):

Summary:

This study reports KRH, a SaCas9 variant computationally engineered via UniDesign to recognize an expanded NNNRRT PAM with substantially enhanced editing efficiency at non-canonical sites. KRH achieves genome- and base-editing efficiencies comparable to or exceeding the evolution-derived KKH variant across multiple human cell types, demonstrating that computational design can effectively remodel PAM specificity while preserving nuclease activity.

Strengths:

The research follows a clear line of reasoning, and the results appear sound. The computational design strategy presented offers a valuable alternative to directed evolution, with potential applicability beyond Cas9 engineering.

<https://doi.org/10.7554/eLife.110906.2.sa1>

Author response:

The following is the authors' response to the original reviews.

Public Reviews:

Reviewer #1 (Public review):

Summary:

This manuscript by Xiong and colleagues presents a compelling validation of UniDesign, a fully computational protein design framework, by using it to engineer a novel, PAM-relaxed variant of Staphylococcus aureus Cas9 (SaCas9) named KRH. The core achievement is the successful de novo generation of a high-performance nuclease (E782K/N968R/R1015H) solely through in silico modeling, without any subsequent experimental optimization or directed evolution. The authors demonstrate that KRH expands the SaCas9 PAM specificity from NNGRRT to NNNRRT, achieving genome editing and base editing efficiencies across multiple human cell types that are comparable to, and sometimes exceed, the well-known evolution-derived KKH variant. The work positions UniDesign not merely as an analytical tool, but as a powerful engine for the generative design of complex molecular functions, offering a scalable and mechanistically insightful alternative to traditional experimental screening.

Strengths:

This is an outstanding manuscript that serves as a powerful proof-of-concept for the next generation of computational protein design. The primary selling point—the raw predictive and generative power of UniDesign—is convincingly demonstrated throughout.

The manuscript shows that the tool can:

(1) successfully navigate a complex sequence landscape to identify a minimal set of three mutations (KRH) that remodel a critical protein-DNA interface;

(2) accurately model and balance the delicate interplay between specific base contacts and non-specific backbone interactions to achieve relaxed PAM specificity;

(3) deliver a final product whose performance is indistinguishable from, and in some cases superior to, a variant that required extensive wet-lab evolution.

The experimental validation is rigorous, thorough, and directly supports the computational predictions. This work will stand as a landmark study for the field, illustrating that computational design has matured to the point where it can reliably generate sophisticated tools for genome engineering.

(1) *Demonstration of Generative Power:*

The most significant finding is that UniDesign, without any experimental feedback, generated a variant (KRH) that matches the performance of the evolution-derived KKH. This is a remarkable achievement. The iterative design strategy—first reducing PAM bias (R1015H), then restoring binding through non-specific interactions (e.g., N968R, E782K)—is a textbook example of rational design, but it is executed entirely by the algorithm. This validates UniDesign's energy function and search algorithm as capable of capturing the subtle biophysical principles governing PAM recognition.

(2) *Mechanistic Insight as a Built-in Feature:*

A key advantage of UniDesign highlighted by this work is its inherent ability to provide mechanistic explanations. The computational models not only predicted which mutations would work (e.g., N968R over N968K in the KRH variant) but also why they work. The structural and energetic analyses showing the bidentate salt bridge formed by Arg968 versus the single bond formed by Lys968 (Figure 4A) is a perfect example of how the tool's output can rationalize functional differences, a level of insight that is rarely attainable from directed evolution campaigns alone.

(3) *Scalability and Accessibility for Engineering:*

The authors explicitly contrast UniDesign's efficiency (minutes to hours per design run) with the computational expense of methods like COMET and the experimental overhead of directed evolution. The improvements to UniDesign v1.2, specifically the mutation-count and sequence-uniqueness penalties, directly address a key challenge in computational design (generating diverse, low-energy point-mutant libraries). This positions the tool as a highly accessible and scalable platform for engineering other CRISPR systems, a point that will be of immense interest to the community.

We sincerely thank the reviewer for the comprehensive summary and the highly positive and encouraging comments on our manuscript.

Weaknesses:

(1) *Title and Abstract Emphasis:*

The title and abstract are effective but could be slightly sharpened to emphasize the primary message. Consider a title like "Fully computational design of a PAM-relaxed SaCas9 variant with UniDesign demonstrates power to match directed evolution." The abstract could more explicitly state upfront that the design was achieved without any experimental iteration.

Thank you for this valuable suggestion. We have revised the title and abstract accordingly to better reflect your feedback.

(2) *Figure 1, Panel M:*

The data points in panel M are currently presented at a font size that makes them difficult to read, particularly the labels for the many triple-mutant variants. This density

obscures the clear identification of the top-performing designs, such as the KRH variant selected for experimental validation. I recommend that the authors increase the font size of all text elements within this panel, including axis labels, tick marks, and data point labels, to improve legibility. If necessary, the panel dimensions can be adjusted or the layout reorganized to accommodate the larger text without compromising clarity. Ensuring this figure is readable is important, as it visually communicates the energetic convergence that led to the selection of KRH.

Thank you for this helpful suggestion. We have increased the font size the Figure 1M, as well as in Figure 1C and Figure 1E, to improve the readability in the revised manuscript.

(3) Generality of the Design Strategy for Other PAM Positions:

The design strategy focused on relaxing specificity at the highly constrained third position of the PAM (the guanine in NNGRRT). How transferable is this specific strategy (i.e., disrupting a key specific contact and compensating with non-specific backbone binders) to relaxing other positions in the PAM or to other Cas enzymes with different PAM-interaction architectures? A short discussion on this point would help readers understand the broader applicability of the "fine-tuning the balance" principle.

Thank you for this insightful question and suggestion. The current study builds upon our previous work on CRISPR–Cas PAM recognition modeling using UniDesign (PMID: 37078688), in which eight Cas9 proteins and two Cas12 proteins (each has a different PAM) were investigated. Our computational results demonstrated that UniDesign can effectively capture the mutual preferences between natural PAMs and native PAM-interacting amino acids (PIAAs). For example, UniDesign accurately predicted the canonical PAMs of SpCas9 and SaCas9 as NGG and NNGRRT, respectively; conversely, given their canonical PAMs, UniDesign successfully recapitulated the corresponding PIAAs in both systems.

These findings provide the foundation for the present study and motivate our selection of SaCas9 as a representative system to explore PAM relaxation, thereby further demonstrating UniDesign's predictive power through experimental validation. Although we did not perform similar PAM relaxation designs for other Cas9 or Cas12 proteins, we believe that the UniDesign framework is broadly generalizable and can be readily extended to these systems. We have included additional discussion to clarify this point and highlight the broader applicability of our design strategy.

Reviewer #2 (Public review):

Summary:

This manuscript describes the fully in silico design of a new variant of Staphylococcus aureus Cas9 (SaCas9) using an improved UniDesign workflow.

The design strategy consists of three sequential steps:

- (1) reducing positional bias at PAM position 3;*
- (2) restoring DNA binding through nonspecific interactions;*
- (3) combining individually favorable substitutions.*

The overall pipeline is conceptually elegant and logically structured, and the genome-editing activity of the designed variants is comprehensively characterized. The resulting KRH variant exhibits relaxed PAM specificity, expanding the targeting range of SaCas9 across diverse cell types. Notably, the KRH variant demonstrates performance comparable to that of the evolution-derived KKH variant, underscoring the effectiveness of the proposed computational design framework.

Strengths:

The design pipeline is entirely computational and does not rely on experimental data for pretraining or iterative optimization.

We thank the reviewer for the concise and accurate summary of our manuscript.

Weaknesses:

The computationally generated KRH mutant differs from the experimentally evolved KKH variant by only a single residue, which may reflect insufficient exploration of the available sequence space.

Thank you for this insightful critique. In the present study, our strategy was not to allow UniDesign to freely explore all 27 mutable positions simultaneously, but rather to constrain the search to point mutations (e.g., double or triple mutants) within the full sequence space (approximately 20^{27}). Even with this constraint, UniDesign effectively samples a substantially large design space compared to traditional protein engineering approaches.

Through iterative design, we observed that only certain residue types became enriched at a subset of positions when identifying effective double mutants. These enriched residues were then systematically combined to generate performance-enhancing triple mutants in an automated manner. Although we ultimately selected the KRH mutant for experimental validation due to its high similarity to the known KKH variant, UniDesign also proposed additional multi-mutants that are distinct from KKH (see Figure 1M).

Reviewer #3 (Public review):**Summary:**

This study reports KRH, a SaCas9 variant computationally engineered via UniDesign to recognize an expanded NNNRRT PAM with substantially enhanced editing efficiency at non-canonical sites. KRH achieves genome- and base-editing efficiencies comparable to or exceeding the evolution-derived KKH variant across multiple human cell types, demonstrating that computational design can effectively remodel PAM specificity while preserving nuclease activity.

Strengths:

The research follows a clear line of reasoning, and the results appear sound. The computational design strategy presented offers a valuable alternative to directed evolution, with potential applicability beyond Cas9 engineering.

We thank the reviewer for the concise and accurate summary of our manuscript.

Weaknesses:

The benchmarking of the UniDesign method is insufficient. How its performance compares to other protein design algorithms, whether the energy function parameters were systematically optimized, and if the design strategy can be generalized to other Cas9 orthologs or genome engineering tasks.

Thank you for this valuable critique. The present study builds upon our previous work on CRISPR–Cas PAM recognition modeling using UniDesign (PMID: 37078688), in which many of these concerns were systematically addressed. In that study, UniDesign was benchmarked against Rosetta, a well-established protein design platform, across eight Cas9 proteins and two Cas12 proteins, each recognizing distinct PAM sequences.

Our results demonstrated that UniDesign effectively captures the mutual preferences between natural PAMs and native PAM-interacting amino acids (PIAAs) across these CRISPR–Cas systems. For example, UniDesign accurately predicted the canonical PAMs of SpCas9 and SaCas9 as NGG and NNGRRT, respectively; conversely, given their canonical PAMs, UniDesign successfully recapitulated the corresponding PIAAs in both systems.

These findings provide the foundation for the present study and motivate our selection of SaCas9 as a representative system to explore PAM relaxation, thereby further demonstrating UniDesign’s predictive power through experimental validation. Although we did not perform analogous PAM relaxation designs for other Cas9 or Cas12 proteins in this work, we believe that the UniDesign framework is broadly generalizable and can be readily extended to these systems. We have incorporated additional discussion in the revised manuscript to address these points and clarify the broader applicability of our approach.

Recommendations for the authors:

Reviewer #2 (Recommendations for the authors):

(1) SaCas9 is highlighted for its AAV compatibility, but the manuscript does not further discuss how the KRH variant may benefit AAV-based genome editing applications. A brief discussion on how expanded PAM compatibility could facilitate target selection in AAV-constrained therapeutic settings would strengthen the translational relevance of the work, potentially reducing the need for split-Cas9 or dual-vector strategies.

Thank you for your helpful suggestion. We have added a brief discussion in the revised manuscript highlighting how the KRH variant’s expanded PAM compatibility may enhance AAV-based genome editing applications. Specifically, this property can broaden the range of targetable genomic sites and may reduce the need for split-Cas9 or dual-vector delivery strategies in size-constrained AAV therapeutic contexts.

(2) The study shows that a fully computational workflow can recapitulate the performance of an evolution-derived variant. A short discussion comparing the scalability and practical advantages of computational design versus directed evolution for future PAM engineering would help emphasize the broader methodological significance of UniDesign.

Thank you for your valuable suggestion. We have added a brief discussion in the revised manuscript comparing the scalability and practical advantages of computational design with directed evolution for PAM engineering. Specifically, we highlight that UniDesign enables rapid and scalable exploration of sequence space without requiring iterative experimental screening, thereby offering a complementary—and in some cases more efficient—approach to directed evolution for future protein engineering applications.

(3) The noticeable variation in editing efficiency across cell types, particularly the lower activity in A549 cells. Could the authors explain why the differences in editing efficiency are so large?

Thank you for this insightful comment. We agree that the variation in editing efficiency across cell types—particularly the lower activity observed in A549 cells—warrants clarification, and we have added a corresponding discussion in the revised manuscript. We attribute this observation to two main factors. First, transfection efficiency varies substantially across cell lines; in our experiments, A549 cells exhibited lower transfection efficiency compared to HEK293T, HeLa, and U2OS cells, which likely contributes to the reduced editing efficiency. Second, the intrinsic performance of genome editing systems can differ across cellular contexts due to variations in DNA repair pathways, including chromatin accessibility and the expression levels of key repair-related genes. Importantly, despite this

cell-type-dependent variability in absolute editing efficiency, the KRH variant consistently outperformed wild-type SaCas9 across all tested cell lines, underscoring the robustness and general applicability of our design.

(4) Given that the computationally generated KRH mutant differs from the experimentally evolved KKH variant by only a single residue, it would be valuable to discuss whether R968 (or saturation mutations at this site) has previously been explored experimentally, and to elaborate on strategies for further expanding the diversity of mutations identified through the computational design framework.

Thank you for your suggestion. We have added a brief discussion in the manuscript noting that, to the best of our knowledge, R968 has not been experimentally characterized prior to this study. It was identified solely through our computational design workflow, highlighting the strength of our approach.

Reviewer #3 (Recommendations for the authors):

(1) During the protein amino acid conformational sampling process in UniDesign, were nucleic acid conformational changes taken into consideration?

Thank you for this question. Nucleic acid conformational changes were not explicitly considered during the protein sequence design stage in UniDesign after the four specific PAM variants (e.g., TTAGGT, TTCGGT, TTGGGT, and TTTGGT) were defined. We consider this assumption reasonable, as the base conformations in these PAM sequences are expected to remain largely stable, with minimal structural variation due to preserved base-stacking interactions.

(2) The authors used a mutation-count penalty to control the number of mutations generated during the design process, which appears to occasionally yield results that exceed the intended limit. Is this an efficient approach? Could the count be controlled more directly by imposing constraints within the design procedure itself?

Thank you for these insightful questions. You are correct that the design process may occasionally yield variants exceeding the intended mutation limit. This occurs because the mutation-count penalty is implemented as a soft constraint, where violations incur a penalty rather than being strictly excluded. Based on our benchmarking, this strategy—combined with the duplicate-design penalty—has been effective in generating multimutant variants with mutation counts close to the desired range. However, we acknowledge that this approach may not achieve optimal efficiency. We are currently developing improved strategies in UniDesign to more directly control mutation counts by incorporating explicit constraints during the sequence simulation process, which we expect will further enhance design precision and efficiency.

(3) Is the new version of UniDesign developed specifically for the Cas9 design task in this study? What are its advantages and disadvantages compared to other state-of-the-art protein design algorithms?

Thank you for this important question. The new version of UniDesign (v1.2) was not developed specifically for Cas9 engineering. Rather, it is intended as a general framework for protein engineering tasks that focus on introducing point mutations to improve protein properties, as opposed to de novo design. Compared to current state-of-the-art protein design methods—many of which are deep learning-based—UniDesign offers distinct advantages and limitations. Deep learning approaches are often highly efficient and powerful but may lack interpretability in their predictions. In contrast, UniDesign is a well-benchmarked, lightweight, physics-based method that provides greater interpretability, allowing users to better understand the underlying basis of the design decisions. On the other hand, a

limitation of UniDesign is that it is less straightforward to incorporate experimental feedback for iterative refinement, such as fine-tuning the scoring function for specific design tasks.

(4) The study employed a three-round design process to obtain the mutants. Is there a conformational correlation between the mutation sites identified in these three rounds? Could this have been accomplished in a single computational run instead of three separate calculations?

Thank you for these insightful questions. We adopted a multi-round design strategy for SaCas9 PAM relaxation because this task inherently involves multi-objective optimization: enhancing PAM compatibility—particularly relaxing base recognition at the third PAM position—while preserving editing activity comparable to wild-type SaCas9. In our view, identifying the key mutations (e.g., E782K, N968R, and R1015H) in a single UniDesign run would be highly challenging due to competing energetic requirements. In the first round, R1015H emerged from single-site mutational scanning as the most favorable PAM-relaxing mutation based on its minimal MAD score. However, this mutation also significantly increased the binding energy relative to wild-type SaCas9 with its native PAM, suggesting a likely reduction in editing activity due to weakened binding. To address this, the second round focused on compensatory mutations. Variants such as E782K and N968R (along with several additional candidates) were identified in the context of R1015H to reduce binding energy and partially restore affinity. In the third round, we further combined compatible mutations from the second round, resulting in variants that more effectively lowered binding energy and restored it to levels comparable to wild-type SaCas9 with its native PAM. Notably, the design objectives in rounds one and two drive binding energy in opposite directions, making it unlikely that all key mutations could be identified simultaneously in a single run. During the design process, we also observed conformational correlations among mutation sites. For example, R1015H can form hydrogen-bonding interactions with residue E993, and we observed multiple alternative mutations at position 993 (e.g., E993S, E993P, E993A, E993G, E993K, and E993R), suggesting local structural coupling between these positions.

(5) In Figure 4D, for the FANCF-1 site, there appears to be a noticeable difference in editing efficiency between KKH-ABE and KRH-ABE. Is this difference statistically significant? If so, please provide an explanation for this observation.

Thank you for this question. For the FANCF-1 site shown in Figure 4D, we performed statistical analyses and found that the differences in editing efficiency between KKH-ABE and KRH-ABE are not statistically significant: $P(A4) = 0.1239$, $P(A10) = 0.0671$, $P(A12) = 0.0942$, and $P(A13) = 0.1349$ (two-tailed unpaired Student's t -test). These results indicate that KRH-ABE and KKH-ABE exhibit comparable editing efficiencies at this site, supporting our overall conclusion that the computationally designed KRH variant achieves performance on par with the KKH variant.

(6) Does the evolutionary term within the UniDesign scoring function bias the designed sequences towards pre-existing protein features?

Thank you for this question. In this study, as well as in our previous work on Cas9 PAM recognition modeling (PMID: 37078688), the evolutionary term in the UniDesign scoring function was completely disabled. Therefore, it does not introduce any bias toward pre-existing protein features in the designed sequences.

<https://doi.org/10.7554/eLife.110906.2.sa0>